MULTIPORT DIFFUSERS FOR HEAT DISPOSAL - A SUMMARY[1]

By Gerhard H. Jirka[2]

Abstract

This paper reviews the fluid mechanical characteristics - as derived from theoretical and experimental studies during the past dozen years - of submerged multiport diffusers used for heat disposal from thermal power plants into the water environment. Foremost among these characteristics is the near field instability produced by such thermal diffusers in typical receiving water conditions. Rather than forming a distinct buoyant plume as is the case for the traditional sewage diffuser, the high discharge momentum of thermal diffusers leads to a flow breakdown with local recirculation zones and full vertical mixing. Stability diagrams for both stagnant and flowing ambient conditions are presented. The flow and temperature fields at larger distances, in the intermediate field, are, in turn, critically dependent upon how the discharge momentum is introduced into the ambient fluid layer. Out of a spectrum of possible diffuser designs three major types have evolved. The unidirectional and staged diffusers are designs which result in concentrated vertically mixed plume motions. The alternating diffuser with appropriate nozzle control generates a stratified flow field outside the unstable near field. Predictive techniques for these basic types are summarized. A typical case comparison illustrates their differences in engineering design and environmental impact.

Preamble

Inasmuch as the elapsed time interval may permit us to gain a proper historical perspective, we have begun to label the 1970's the "environmental decade". Indeed, this characterization seems entirely justified. A series of environmental disasters in the late sixties - Santa Barbara oil spill, Cuyahoga River burning, Lake Erie fish kills - spurred the environmental

[1]The Eleventh John R. Freeman Memorial Lecture. Presented at a joint meeting of the Hydraulics Group of the Boston Society of Civil Engineers Section and the M.I.T. Student Chapter of the American Society of Civil Engineers, at M.I.T., April 21, 1982.

[2]Associate Professor, School of Civil and Environmental Engineering, Cornell University, Ithaca, New York.

movement, and led to a surge in public awareness and, ultimately, resulted in sweeping legislations with the intent of controlling the human impact on the environment. Much of this process, though long overdue, was impulsive, hasty and narrowly focused. Frequently, it lacked a scientific base, a tradeoff between one environmental impact versus another and due consideration for conflicting societal objectives, such as economic costs. The concurrent energy crisis exacerbated the latter conflict. Consequently, considerable "re-interpretation" and "adjustment" of earlier legislation took place in the latter part of the decade. Undoubtedly, this development will continue. A sound and balanced environmental policy which is grounded in a mature public perception of all inherent conflicts and trade-offs is the hope for the future.

The research and development of the submerged multiport diffuser technology for waste heat management of steam-electric power stations is closely linked to the environmental history of the 1970's. With the advent of large capacity central power stations it became evident that the traditional surface discharge scheme which used to be the dominant once-through heat disposal technique was unsatisfactory in most receiving water environments: it seemed to result in large regions of raised surface temperatures and often with significant shoreline impact. Thus, in the late sixties and early seventies the multiport diffuser was heralded by the engineering community as the solution to the thermal pollution issue. However, this early impetus for technology development and implementation was soon waning when the following obstacles emerged. First, several state environmental agencies issued overly restrictive temperature standards and mixing zone requirements; at least, they appear so in retrospect in the light of accumulated experience and scientific evidence. This led to exceedingly costly diffuser designs and thus diminished the main economic advantage of once-through heat disposal techniques over closed-cycle cooling towers.

Second, design engineers and regulatory reviewers were frustrated by the absence of simple predictive mathematical techniques for diffuser design and/or design verification. Early attempts to draw on the seemingly related problem of submerged diffusers for sewage disposal proved a dismal failure when compared to the few available experiments. Thus, design had to proceed with time-consuming and costly hydraulic model studies. Third, the Federal Water Pollution Control Act Amendments of 1972 defined thermal discharges as a pollutant. Therefore, the Amendments' goal of zero pollutant discharge by 1985 appeared to suggest the elimination of once-through heat disposal schemes. Subsequent studies by the U.S. Environmental Protection Agency proposed the mechanical draft evaporative cooling tower as the "best available" control technology. But, just as the extreme philosophy of "zero pollutant discharge" into water has come under increasing attack for its lack of a balanced consideration of air, land, energy and water resources and of economic consequences, there has been an increasing use of several important exemptions of the 1972 Amendments. In essence, these exemptions allow the utilization of once-through schemes if systematic ecological studies of the receiving water demonstrate that the discharge assures "the protection and propagation of a balanced, indigeneous community of fish, shellfish and wildlife". This trend toward a site specific assessment methodology, rather than a strict advocacy of one technology versus another one, is indeed a healthy one. Thus, recent years have seen a continued and renewed interest in multiport diffusers. A recent study (36) on the ability of once-through systems to comply with typical thermal standards - note, that this compliance can, of course, only be seen as a surrogate to a systematic assessment of the site-specific ecological impact - concluded: "Submerged multiport diffusers were found to provide the greatest likelihood of meeting thermal standards in all receiving environments" (i.e. rivers, lakes, estuaries and coastal waters).

This writer anticipates that, in the future, submerged multiport diffusers will be the preferred heat disposal alternative for central power stations, whenever a sufficiently large water body is available near the plant site. Thus, it is the purpose of this paper to summarize recent analytical and experimental results on thermal diffuser mechanics together with some operational experience on completed installations. It is shown that there exist several types of thermal diffusers with rather divergent characteristics. An understanding of these types is a prerequisite for the design engineer to use thermal diffusers as a truly flexible tool for environmental management.

I. Introduction and Definitions

A multiport diffuser is defined as a linear structure consisting of many closely spaced ports or nozzles which inject a series of turbulent jets at high velocity into the receiving water. These ports may be attached as risers to an underground pipe or, simply, may be openings in a pipe lying on the bottom. This diffuser pipe, usually of varying diameter to insure the desired flow distribution through the individual ports, is connected by means of a feeder pipeline to the onshore power plant.

The interplay of diffuser location, design details and ambient conditions, as indicated in Fig. 1, determines the resulting temperature and velocity fields in the receiving water. An adequate prediction of these fields is a basic requisite for further environmental impact analysis of a proposed installation. Most usefully, such predictions are carried out in a "zonal approach", that is, subdividing the expected flow field into zones of unique characteristics. Different such subdivisions made on an ad-hoc basis may be found in the literature. For the present purpose, we will use subdivision into three zones: the near field, usually a highly

three-dimensional zone, in which the individual jets interact, effectively entrain, and diffuse their momentum into, the surrounding fluid; the intermediate field in which large scale motions and circulations - often in form of a distinct "diffuser plume" - are set up with additional, though less vigorous, mixing and buoyant spreading; and the far field in which advection and turbulent diffusion by ambient currents dominate. In essence, the far field constitutes a passive dispersal process. Its analysis which follows the traditional pattern of Eulerian or Lagrangian-type transport models will not be considered herein. Rather, attention is restricted to the active dispersal processes which make up the near and intermediate field zones.

That the active dispersal zones produced by modern large heat diffusers can extend over considerable distances and can cause a significant influence on the ambient hydrologic structure is shown in the following illustrative example. The example also serves to document some of the fundamental fluid mechanical differences between "thermal diffusers" and "sewage diffusers". We consider a coastal city with a population of one million. Given U.S. national averages, the city's installed electric capacity is of the order of 2000 MW and its flowrate for combined sewage and stormwater runoff is of the order of 200 million gallons per day. Assuming a central station nuclear power plant with once-through cooling and a single regional sewage treatment facility, Table 1 gives the respective discharge flow rates, Q_o. Several installed or planned outfalls of either category have discharges of this magnitude and larger. We note that the cooling water flowrate exceeds the sewage flow by a factor of 10. Referring to Fig. 1, it can be seen that multiport diffusers exhibit a tantalizing amount of detail, e.g. discharge velocity U_o, port spacing ℓ, vertical port angle θ_o, horizontal port orientation β, all of which may be variable along the diffuser axis. For the moment, we neglect much of this detail and concentrate on the two flow parameters which we ex-

pect to have major influence on the global dynamic characteristics of the diffuser flow field. Those are the total buoyancy flux, P_o, and the total momentum flux, M_o, both expressed in kinematic units, $P_o = Q_o \frac{\Delta\rho_o}{\rho_a} g$ and $M_o = Q_o U_o$, where $\Delta\rho_o = \rho_a - \rho_o$, ρ_o = discharge density and ρ_a = ambient density. Because of a tenfold discrepancy in the relative density differences which is due to the fresh-salt water interaction in one case and the thermal expansion in the other, the buoyancy flux is in fact the same for both diffusers. It corresponds roughly to the buoyant weight of a volume of 0.2 m^3 (7 ft^3) released per second. On the other hand, given a typical discharge velocity of 5 m/s (9.8 ft/s) the momentum flux for the thermal diffuser is ten times larger. The further implications of these flux parameters must be considered in the context of diffuser site selection. Sewage diffusers require deep sites, H of the order of 50 m (163 ft), because health regulations impose rather high near-field dilutions (order of 100 and more). The required near-field dilution for thermal diffusers is much lower, 5 to 10, so that the diffuser can be located in much shallower water, H of the order of 10 m (33 ft). For a typical diffuser length, L_D = 500 m (1640 ft) the distributed momentum flux which impacts the available water column, L_D H, hence $M_o/(L_D H)$, is fifty times larger for the thermal diffuser. Hence, much stronger accelerations take place within the receiving water. Although with the present global analysis we cannot predict the induced velocities - this will depend, as is shown later on, on some of the details presently omitted, e.g. port orientation - we can expect the induced velocities to be of order $[M_o/(L_D H)]^{1/2}$. Using an ambient velocity of 0.3 m/s(1 ft/s) as a convenient reference velocity for offshore currents of tidal, wind driven or inertial origin, we find that the thermal diffuser induces velocities of equal magnitude while the

velocity field induced by the sewage diffuser is probably not detectable in the signal noise of the ambient current.

Hence, the following conclusions can be drawn on the basis of these rather general considerations: 1) The near field mixing of a thermal diffuser is strongly influenced by its momentum flux. For a sewage diffuser, however, the role of the momentum flux is minor and its mixing is governed by its buoyancy flux as is known from previous work (e.g., 26). 2) The intermediate field of the thermal diffuser is characterized by large induced velocities which can be expected to persist over considerable distances and to cause a modification of the ambient coastal circulation system. The intermediate field dynamics are largely non-existent in sewage diffuser discharges - except for some buoyant collapse motions - and its overall flow field is given by a direct transition from near field (buoyant plume) processes to far field processes. This radical departure of thermal diffuser analysis from established procedures for sewage diffusers is further highlighted in the remainder of this paper. We review studies of the near field behavior (Section 2) and of the induced circulation patterns for different diffuser types (Sections 3 to 6) both of which are fundamental to the understanding of the active dispersal phases of a thermal diffuser. Finally, some design implications are discussed (Section 7) and the paper concludes with suggestions for future work.

2. Near Field Stability

It is intuitively obvious that, depending on the role of buoyancy, the injection of turbulent jets into an ambient unstratified fluid layer can generate radically different flow patterns in the immediate discharge vicinity, the near field. In the absence of buoyancy, on the one hand, we expect that the discharge will cause recirculating eddies within the limited

layer as the jet is deflected by opposite fluid boundaries. Discharges with strong buoyancy, on the other hand, are expected to rise in form of a bouyant jet toward the fluid surface and to spread along the surface in form of a well defined layered flow. Hence, the object of the near-field stability analysis is to predict under what combinations of discharge and ambient characteristics the near field will be stable or unstable. A stable near field is defined as one in which a buoyant surface layer is formed which does not communicate with the initial buoyant jet zone, as illustrated in Fig. 2a. The near field is defined as unstable whenever the layered flow structure breaks down in the discharge vicinity, resulting in recirculating zones or mixing over the entire water depth, as shown in Fig. 2b.

Whilst the general flow field of a diffuser is always a highly three-dimensional one, we introduce for purposes of the stability analysis a two-dimensional channel model (see Fig. 3). This assumes that the flow field in the diffuser center portion is approximately two-dimensional. Furthermore, the details of the individual jets with initial diameter D and spacing ℓ are neglected by assuming an equivalent slot jet with slot width $B = (D^2\pi)/(4\ell)$ on the basis of equivalency of momentum flux per unit diffuser length. This equivalent slot concept has been shown to be sufficiently accurate representation of the mixing of merging individual jets (14,23,25) if attention lies in the region after merging. For the tangent, $k \approx 0.5$, of the total angle of spread of a round turbulent jet (41), the condition for merging would be $\ell/H < 0.5$ for the extreme case of a vertical discharge. However, the results derived in the following have been found reliable for even larger spacings.

The major dynamic elements in this two-dimensional framework which affect the near field stability of a discharge from slot width B and initial angle θ_o into a layer depth H are then the buoyancy flux per unit length, p_o =

$U_o B\, g'_o$, in which $g'_o = \frac{\Delta\rho_o}{\rho_a} g$, as a stabilizing element and the momentum flux per unit length, $m_o = U_o^2 B$, as a destabilizing element. Furthermore if an ambient crossflow exists in the direction of the channel then its momentum flux per unit length, $m_a = u_a^2 H$, also will play a destabilizing role. These two destabilizing elements are considered separately.

2.1 Stagnant Ambient:

The premise of the stability analysis is to define a mathematical model for the stable discharge configuration which includes the horizontal surface layer spreading after jet impingement. Then, decreasing the buoyancy flux in the model will eventually lead to an instability and breakdown of the layered structure. This condition, the stability criterion, is attained when the inertia forces overcome the stabilizing effect of buoyancy. Details of this analysis and its experimental verification have been given elsewhere (21, 23, and 24 for the special case of vertical discharge, $\theta_o = 90°$) and a summary only is given here.

Experimental data (e.g. Fig. 2b) and basic stratified flow theory suggest that under stable near field conditions the following structure exists in the two-dimensional channel configuration: (i) A buoyant jet region in which the discharge entrains ambient water while rising toward the surface. This region is analysed using Morton et. al's (35) entrainment concept with a variable entrainment coefficient which depends on the local densimetric Froude number of the jet and on the local jet angle. For the special case, $\theta_o = 90°$, this variable entrainment approach is shown to agree with the constant buoyant jet spreading analysis as proposed by Schmidt (43) and Abraham (1) which appears to be in closest agreement with available data. (ii) A surface impingement region provides a transition between the buoyant jet flow which has a strong vertical component and the horizontal spreading motion. A control volume analysis which includes continuity and momentum conservation and allows for

internal energy dissipation in the abrupt change of flow direction gives the geometric and dynamic characteristics of the initial spreading layer. In particular, it is found that the layer (in both $\pm$ x directions) always spreads supercritically in the sense of an internal densimetric Froude number defined on basis of layer velocity, thickness and buoyancy. (iii) An internal hydraulic jump region links the supercritical counterflow system after impingement with the ensuing subcritical counterflow region. Thus a rapid change in flow state takes place which is analysed using the momentum conservation principle. These three regions together constitute the near-field zone while the gradually varying stratified counterflow is in fact an intermediate field process which connects the discharge to the surrounding large basin, i.e. the inert far-field.

The complete analysis of the three near field regions indicates that a transition to a stable intermediate field flow is possible only for sufficiently high discharge buoyancy. For smaller values of discharge buoyancy no conjugate solution can be found which would satisfy the momentum conservation equation governing the internal hydraulic jump. Consequently, a flow breakdown may be anticipated which leads to dissipation of the excess momentum in the form of a recirculating eddy zone.

The theoretical predictions of the stability criterion is given in Fig. 4 using the parameter space of a discharge slot densimetric Froude number $F_s = m_o^{3/4} p_o^{-1/2} B^{-3/4}$ and relative depth H/B with the discharge angle θ_o as the third variable. This stability diagram indicates a stable near field for low F_s and large H/B so that a stable discharge can be labeled synonymously as a "deep water" discharge. The parameter range of large F_s and low H/B, on the other hand, is unstable, i.e. a "shallow water" discharge. The symmetrical discharge condition, $\theta_o = 90°$, is more stable than asymmetric discharges,

$\theta_o < 90°$, which result in a net horizontal acceleration of the ambient flow. Experiments over a wide parameter range are in good agreement with the theoretical criteria (see Fig. 4).

For the asymptotic condition $H/B \to \infty$, the stability criterion is closely represented by a simple best-fit expression

$$\frac{H}{B} = 1.84\ F_s^{4/3}(1 + \cos^2\theta_o)^2 \qquad (1)$$

This is a good approximation for $H/B > 200$. This fact suggests to neglect the slot width as a significant parameter, $B \to 0$, by combining F_s and H/B into a new parameter $m_o/(p_o^{2/3}H) = F_s^{4/3}/(H/B)$. Using Eq. 1, the stability criterion for a line buoyant jet in confined depth is given by a convenient two parameter expression

$$\frac{m_o}{p_o^{2/3}\,H} = \frac{0.54}{(1 + \cos^2\theta_o)^2} \qquad (2)$$

It is interesting to apply this criterion to the earlier comparison between sewage and thermal diffusers given in Table 1. We find $m_o/(p_o^{2/3}\,H) =$ 0.08 and 3.84, respectively. Thus, typical sewage diffuser operate clearly in the stabledomain while thermal diffusers have an unstable near field. These points are also included in Fig. 5 as "S" and "T", respectively. Hence, simple buoyant jet analyses which in essence assume an infinite receiving water body suffice to calculate the mixing characteristics of sewage diffusers. Conversely, altogether different techniques must be employed in the design of thermal diffusers where a distinct jet zone does no longer exist due to the flow breakdown in the near field.

2.2 Ambient Crossflow:

The additional destabilizing effect of an ambient crossflow of velocity u_a which is superimposed on the diffuser operating in the two-dimensional channel conceptualization can be represented by another parameter $m_a/(p_o^{2/3} H)$. So far, a detailed analytical development of the stability criterion for this situation is wanting. A simple estimate for the momentumless discharge case, $m_o/(p_o^{2/3} H) \approx 0$, can be given using a result of stratified flow theory which indicates that layered flow is only possible if the densimetric Froude number $F_a = q_a/(g' H^3)^{1/2}$ is less than a limit value $F_a^* = 1$ where q_a is the net discharge and $g' = \frac{\Delta\rho}{\rho_a} g$ the buoyancy difference between the layers. Several experimental results (e.g. 15) indicate that, in practice this limit is even lower, $F_a^* = 0.6$ to 0.7, apparently because of the neglect of vertical accelerations in the theory. However, if the stable stratified discharge flow is experiencing this limiting breakdown condition leading to vertical mixing, then $g' = g'_o/S$ where S is the mixing ratio given by $S \approx q_a/q_o$, approximately. Appropriate substitution and use of $F^* = 0.65$ yields an estimate for the stability criterion

$$\frac{m_a}{p_o^{2/3} H} = (F_a^*)^{4/3} = 0.56 \qquad (3)$$

Thus, comparing Eq. 3 with Eq. 2 it can be seen that the discharge momentum flux m_o plays a quantitatively similar destabiliizing role as the horizontal ambient momentum flux, m_a. On the other hand, Eq. 2 indicates that the tendency to instability is further increased if the discharge momentum also has a horizontal component, $m_o \cos\theta_o$. In situations involving both horizontal momentum flux elements, m_a and $m_o \cos\theta_o$, the separate destabilizing roles of the total horizontal momentum flux, $m_a + m_o \cos\theta_o$, and the total discharge

momentum flux, m_o, - both scaled by the stabilizing factor $p_o^{2/3}H$ - can then be displayed in a general stability diagram as shown in Fig. 5. Furthermore, given the numerical constants of Eq.s 2 and 3 an approximate stability criterion for small slot width, $H/B \to \infty$, can be proposed as

$$\frac{m_o}{p_o^{2/3} H} + \frac{m_a + m_o \cos \theta_o}{p_o^{2/3} H} = 0.54 \qquad (4)$$

Eq. 4 is plotted in Fig. 5 together with Eq. 2. The latter expression would be valid only for the case of $m_a = 0$ but finite $m_o \cos \theta_o$ and is thus linked to the lower 45° sector of the plot. In that case the disagreement between both equations is given by the factor $(1 + \cos^2 \theta_o)^2/(1 + \cos \theta_o)$ which takes on a maximum of 2 for $\theta_o = 0°$. However, comparison with extensive experiments in Fig. 5 indicates that despite this discrepancy Eq. 4 seems to be a good representation for diffuser near field stability in the general case of both discharge induced and crossflow induced destabilizing effects.

Several comments regarding Fig. 5 are in order. The scales on both axis are distorted by taking the fourth root of the parameters in order to display equally the stable and unstable range. Experiments on discharge stability in the presence of ambient crossflow have been performed by Cederwall (14), Jirka and Harleman (23), Buhler (13) and Roberts (39). In addition, some of the data on stagnant ambient conditions, already given in Fig. 4, has been included in Fig. 5. Among Cederwall's experiments on vertical discharges only those data points which he had labeled as "jet or plume-like patterns" were considered as stable near field. Stratified downstream conditions in other experiments are judged to be intermediate field phenomena as will be mentioned further below. The momentum in Roberts' experiments was computed by assuming a fully developed pure plume at the slot exit. Fig. 5 also includes the

operating conditions (see Table 1) for sewage and thermal diffusers, with and without ambient flow, thus points "S", "SA" and "T", "TA", respectively. Even the otherwise stable sewage diffuser discharge experiences a local flow breakdown in the diffuser vicintiy under the effect of crossflow. This has been the result of the sewage diffuser studies by Buhler in a two-dimensional model and by Roberts in the fully three-dimensional domain.

In summary, these stability analyses demonstrate that thermal diffusers always have an unstable near field. Hence, analysis techniques which are altogether different from the simple buoyant jet theories for sewage diffusers (at least in the stagnant range) must be employed to determine the mixing capability of thermal diffusers. Note, however, that the near field instability relates to the immediate vicinity (of the order of several water depths) of diffusers. The flow field at larger distances can sometimes restratify due to intrusion processes. However, these are intermediate field processes - as analysed in later sections - which are governed by the overall larger scale geometry rather than the discharge characteristics. This aspect underlies inconsistencies seen in the earlier discharge stability criteria by Cederwall (14) and Argue and Sayre (9).

3. Major Types of Shallow Water Diffusers

Using merely two-dimensional analyses so far, we have shown that shallow water diffusers are dominated by their discharge momentum. Since momentum is a directed (vector) quantity, we must expect, therefore, that the diffuser dynamics in the general three-dimensional case (see Fig. 1) will critically depend upon how that momentum is introduced. This is controlled by the vertical (θ_o) and horizontal angle (β) of the diffuser nozzles. Using the line diffuser concept from now on (i.e. a slot diffuser with $B \to 0$), the

diffuser boundary conditions for the three-dimensional problem are the three components of momentum and buoyancy flux which are variable along the diffuser axis

$$\vec{m}_o(y) \quad , \quad \vec{p}_o(y) \qquad \text{at } -\frac{L_D}{2} \leq y \leq \frac{L_D}{2} \tag{5}$$

in the coordinate system of Fig. 1. These and other boundary conditions together with the governing equations (e.g. the turbulent Reynolds equations) which are not stated here would give the general problem statement. No solutions to that general problem are presently known or easily derivable, even for simpler cases such as the unbounded ($x,y \to \pm\infty$), constant depth, stagnant shallow layer. Making yet another simplification, namely neglecting the buoyancy flux, $\vec{p}_o \to 0$, and hence the possibility of restratification in the intermediate field that has been alluded to earlier, allows one to formulate - by means of vertical integration - a purely two-dimensional problem with the two-component momentum vector

$$\vec{m}_o(y) \cos \theta_o \qquad \text{at } -\frac{L_D}{2} \leq y \leq \frac{L_D}{2} \tag{6}$$

as the diffuser boundary condition. This includes the tacit, yet tenuous, assumption that the vertical component of the momentum flux gets dissipated (rather than re-directed) in the near-field process (see Section 6). In any case, the ensuing governing equations (with appropriate bottom friction terms) would then describe a class of problems which may be labeled as "momentum induced circulations in a shallow fluid layer" (or, alternatively, in two-dimensional space) which has many corollories in classical fluid mechanics. In particular, scaling analyses of the equation indicate that for moderate distances, $(x,y)/L_D < 1$, frictional effects are indeed negligible, so that one

may conceive of using fully inviscid flow theory, e.g. a superposition of line momentum sources (dipoles). Still, that approach has considerable pitfalls and leads to erroneous results as a later example will show.

Thus, a generally valid diffuser theory for arbitrary discharge conditions has not been established as yet. Instead, we will concentrate the further analysis on three special diffuser types which have emerged in design practice during the past decade. These types (see Fig. 6) are classified by their nozzle angles β and θ_o as: 1) Unidirectional diffuser, $\beta = 90°$, $\theta_o \approx 0°$. 2) Staged diffuser, $\beta \approx 0°$, $\theta_o \approx 0°$, and 3) Alternating diffuser, $\beta = \pm\beta(y)$, i.e. a variable orientation along the diffuser axis with every other nozzle pointing to a different side, θ_o = variable, i.e.not a preferred horizontal orientation. The important distinction between these types lies in the fact that, for a control volume enclosing the entire diffuser, the first two types have a net horizontal momentum input with strong induced currents, while the alternating diffuser has zero net horizontal momentum, with lesser induced currents whose magnitude will, presumably, depend upon $\beta(y)$. The performance of each of these types under the influence of an ambient current will depend upon the alignment angle, γ, between diffuser axis and current direction. We distinguish between two extreme cases: 1) Parallel diffuser alignment, $\gamma \approx 0°$, and 2) Perpendicular diffuser alignment, $\gamma \approx 90°$.

The following analyses for the three diffuser types have this common base: (i) Near-field is unstable. (ii) Constant ambient depth. (iii) No shoreline effect ($x,y \to \pm\infty$). (iv) Line diffuser approximation. (v) Stagnant conditions which, in terms of mixing, are the critical worst case are considered first, followed by an extension to crossflow conditions. Deviations from these common assumptions will be treated on an ad hoc basis.

4. Unidirectional Diffusers

Probably, the earliest designs for unidirectional diffusers in a coastal environment were for the FitzPatrick Station (45) on Lake Ontario and the Zion Station (28) on Lake Michigan. Unidirectional diffuser designs in rivers which pose rather different constraints were initially proposed for the Browns Ferry Station (46) on the Tennessee River and the Quad Cities Station (19) on the Mississippi.

4.1 Stagnant Ambient

Synopsis of the flow field: Detailed experimental studies (e.g. Fig. 7a) have shown that the "plume" - an intermediate field phenomenon in the present terminology - produced by a unidirectional diffuser has a distinct structure as indicated in Fig. 7b. In steady state the momentum flux at the diffuser line accelerates the ambient fluid from large distances behind the diffuser and also provides a pressure discontinuity across the diffuser line, i.e. the local surface elevation h^- upstream is depressed, $h^- < H$, and downstream, $h^+ > H$. Flow separation at thediffuser ends causes the flow downstream to accelerate even further, that is, the excess pressure head is converted into kinetic energy. Thus an acceleration zone, or "slipstream", is formed immediately downstream, much like a two-dimensional analog to the flow downwind from a propeller (e.g. Prandtl, 37). Although the slipstream motion is an essentially inviscid phenomenon, the plume is further affected in two ways by its real fluidcharacter. First, the velocity discontinuity at the slipstream boundary gives rise to lateral diffusion effects leading to side entrainment similar to ordinary jets. Second, turbulent bottom friction will lead to gradual dissipation of the plume momentum, and thus deceleration and ultimate stagnation. This provides the transition to far field processes. The unstable near field in Fig. 7 is that highly three-dimensional zone in which the individual jets (or the line jet) become vertically mixed over the

water column. Its extent in the x-direction is about 5H to 10H (30) and thus negligible for long diffusers $L_D/H \gg 1$. In total, the mixing characteristics of the diffuser are influenced by back entrainment, due to the bulk acceleration of the ambient fluid, and by side entrainment, due to lateral diffusion.

Slipstream analysis: Straightforward scaling (4, 30) of the governing vertically averaged momentum equations using L_D as the characteristic horizontal length scale and typical estimates for bottom friction and lateral diffusivities proves that the acceleration zone flow is, indeed, governed by inviscid dynamics. This raises an interesting temptation, namely to use potential theory with a simple superposition of dipoles of strength m_o/Hdy along $-\frac{L_D}{2} < y < \frac{L_D}{2}$. Integration gives then a potential flow field given by the consisting of two vortices located at the diffuser end, hence describing a recirculating flow. What is wrong with this model as it obviously does not agree with our observations (Fig. 7)? The answer is, of course, provided by basic boundary layer theory. Thus, the intense shearing action in the near field - here, in fact, the scaling length ought to be much smaller - generates sufficient vorticity that the decelerating and expanding flow which is implied by the two-vortex model cannot be sustained. The flow separates at the point of minimum pressure, that is, the diffuser end, and forms an entirely different downstream zone. However, that zone can be described again by inviscid theory, albeit with different boundary conditions and a different Bernoulli constant. An interesting analogy to the present situation is given by converging-diverging flow geometries such as an orifice in a pipe where a continuous potential flow theory fails and separation at the orifice throat is triggered by vorticity generation at the solid wall.

Adams (4, see also 30) was the first to analyse the contracting slip stream by using the elements of propeller theory (37), namely Bernoulli equa-

tions for the approach flow ($x < 0^-$) and the contracting flow ($x > 0^+$) and a momentum equation for the pressure discontinuity across the diffuser line ($0 < x < 0$). The result can be written as

$$u_N = \left(\frac{2\, m_o}{H}\right)^{1/2} , \quad \sigma = \frac{1}{2} \tag{6}$$

where u_N and $L_N = \sigma L_D$ are the slipstream velocity and width at the fully contracted uniform downstream section. The total discharge in the slipstream is therefore

$$Q_N = \left(\frac{m_o H}{2}\right)^{1/2} L_D \tag{7}$$

and a bulk dilution S can be defined by relating Q_N to the discharge flow $Q_o = q_o L_D$ or to the excess temperature flux $J_o = Q_o \Delta T_o$ (a passive tracer in this case)

$$S = \frac{\Delta T_o}{\Delta T_N} = \frac{Q_N}{Q_o} = \frac{1}{q_o}\left(\frac{m_o H}{2}\right)^{1/2} \tag{8a}$$

where ΔT_N is the excess temperature of the slipstream. From a design viewpoint, it is often interesting to relate this to the manifold geometry

$$S = \left(\frac{\ell H}{2 a_o}\right)^{1/2} \tag{8b}$$

where $a_o = D^2\pi/4$ is the individual nozzle area. This one-dimensional theory does not give any further results on the slipstream properties. A detailed two-dimensional analysis was developed by Lee, Jirka and Harleman (30, 31) using a diffuser boundary condition of uniform velocities and uniform accelerations in the x-direction. A complex mapping transformation into the

hodograph plane predicted the detailed geometry and velocity distribution. Most notably, the asymptotic slipstream values given by Eq. 6 are essentially approached within one half diffuser length, $x \approx L_D/2$, and the angle of separation at the diffuser end is 60° with respect to the x-axis. These results and the predicted slipstream velocity distribution appear to be in good agreement with observations (30) although sufficiently detailed exerimental data on slipstream properties still are limited.

The bulk dilution parameter S, Eq. 8, is therefore an important predictor for the initial back entrainment characteristics of a unidirectional diffuser. It is usually easily observed as it can be measured within a uniform temperature plateau, ΔT_N, downstream from the diffuser. Existing observations agree well with theory as shown in Fig. 8.

Complete intermediate field plume: Even though the real fluid effects are of lesser importance within the initial acceleration zone, their incremental influence dominates the diffuser plume at larger distances. The analysis by Lee et al. assumes a boundary layer plume structure (see Fig. 9) in which the initial slipstream is surrounded by a narrow, but growing, diffusion zone until, at a distance x_I, the potential core region has been fully erased. The governing integral equation set is

$$\frac{dQ}{dx} = 2\,\alpha\, u_c H, \qquad \frac{dM}{dx} = \frac{dP_e}{dx} - \frac{\lambda}{H} M, \qquad \frac{dJ}{dx} = 0 \tag{9}$$

with the plume cross-sectional flux quantities defined as

$$Q = H \int_{-\infty}^{\infty} u\, dy, \qquad M = H \int_{-\infty}^{\infty} u^2\, dy, \qquad \text{and } J = H \int_{-\infty}^{\infty} u\, \Delta T\, dy \tag{10}$$

In Eq. 9 P_e represents the integrated excess pressure which is evaluated from the slipstream solution and vanishes once the asymptotic condition has

been reached ($x \gtrsim L_D/2$), λ is a friction factor related to f_o, the Darcy-Weisbach wall friction factor, $\lambda = f_o/8$, u_c the plume maximum velocity and α an entrainment coefficient. Assuming self-similar diffusion profiles of the Gaussian type, which, for $x < x_I$, are combined with constant core values, Eq.s 9 and 10 can be readily integrated to predict the plume evolution with distance x. Fig. 10 summarizes two important aspects of the solution, namely the plume momentum flux and volume flux, the latter scaled by the initial back entrainment value, Q_N. The solutions depend upon a friction parameter $\Phi = \lambda \frac{L_D}{H}$. Fig. 10a shows the initial increase in plume momentum in the acceleration zone and the gradual dissipation due to bottom friction. The frictional length scale x_f at which the diffuser momentum has decreased to 1/e of its initial value is

$$x_f/L_D \sim \Phi^{-1} \tag{11}$$

This loss of plume momentum also puts a limit on the additional side entrainment - for a regular momentum jet without bottom friction would entrain ad infinitum - which is given (if $x_f >> x_I$) by

$$\frac{Q_{max}}{Q_N} \sim \sqrt{2}\ (1 + \frac{4\ \alpha}{\sqrt{\pi}\ \Phi})^{1/2} \tag{12}$$

with $\alpha = 0.068$ for a momentum jet and the numerical values corresponding to the Gaussian profiles (30). For comparison, Fig. 10 also includes the behavior of a regular frictionless momentum jet with equal momentum flux, initial width L_D and discharge Q_N. Another effect of bottom friction is the increasing lateral growth of the plume.

These essential features of Lee et al.'s plume analysis are well verified by experimental data (30, 31). Of particular interest for environmental impact analysis is the prediction of excess isotherm areas, scaled by L_D^2, as given in Fig. 11 in which $\Delta T_N = \Delta T_o/S$. The plot shows good agreement and sensitivity to the frictional parameter Φ. The laboratory data describe relatively short diffuser lengths and hence lie below the theory for small A/L_D as the three-dimensional near field effects prevent a full vertical mixing of the plume and thus establishment of the expected temperature plateau. Fig.s 8 and 11 also give field data for the FitzPatrick Station, apparently the first coastal diffuser installation for which operating experience has become available.

A two-dimensional channel analysis: Some lessons about diffuser performance can be gleaned from the simple two-dimensional model that had been sketched in Fig. 3. This model has been used in an early diffuser study (18) to evaluate the diffuser mixing capacity. The analysis uses the energy equation for a streamline which commences far upstream and ends well downstream. The head losses along the streamline, as it passes through the channel, are balanced by the diffuser generated head differential. Thus, the diffuser acts much like a ducted axial flow pump. The predicted dilution is (23)

$$S_{2D} = \frac{1}{q_o} \frac{1}{\{1 + \sum k\}^{1/2}} (2\, m_o H)^{1/2} \qquad (13)$$

which may be compared to Eq. 8a for the actual three-dimensional case. The constants in the wavy bracket are of interest: The value of unity is the exit loss coefficient, which describes the complete loss of channel flow energy once it re-enters the surrounding reservoir while $\sum k$ stands for the sum of the internal losses, such as entrance flow separation and internal friction. Analysis of channel laboratory data indicated that $\sum k = 0.25$ to 0.5. Thus, if

we assume optimistically $\sum k \approx 0$, then the channel diffuser would have an initial, back entrainment related, dilution capacity twice as large as its three-dimensional analog. The poorer performance of the latter is, of course, due to the fact that a larger fraction of the diffuser energy is stored as kinetic energy in the high velocity slipstream and does not do useful back entrainment work. The more vigorous dissipation leads, however, to a more effective side entrainment process at larger downstream distances. In any case, if maximization of the initial bulk dilution is of interest for a given design, one might consider to "control" the slipstream contraction by placing guiding walls - possibly extending only over a fraction of the water depth - at both diffuser ends and even at regular intervals along the diffuser. No such designs have been made and their cost effectiveness remains to be studied. It is interesting to observe that qualitatively similar proposals for ducted propeller design have been made recently for more efficient energy extraction systems for wind (47) and ocean current energy (34). Another control possibility was explored by the writer (23), namely fanning out of the diffuser nozzles - roughly as indicated in Fig. 3 - to provide momentum in $\pm$ y-direction and thus counteract the contraction tendency. However, improvements in terms of the reduced dilution turned out to be marginal ($\approx$ 10%), much less than the optimal factor of two. This failure appears to be related to the natural tendency of diffuser induced circulations to "lock into" certain patterns as will be further discussed in Section 6.

Recirculation tendencies: From a large scale point of view the diffuser action in the constant depth fluid layer can be considered as a source-sink interaction. The source is given by the stagnation region, while the major sink exists at the diffuser line. This raises the possibility of recirculation, that is the return of heated water back to the diffuser and, hence, an unsteady temperature build-up. This problem was addressed by Lee et al. (32) using order of magnitude arguments. The results, show that the

recirculation potential may be significant for laboratory studies in which the limited basin boundaries may impose another constraint. But it is of little importance in actual field applications where such far-field effects as heat loss and diffusion are acting much faster than the recirculative advection.

Restratifiction in the intermediate field: Thus far, fully mixed conditions have been assumed. In view of our earlier stability considerations, this clearly holds in the early portions of the plume. However, given the finite buoyancy flux, at some point a restratification must be expected to occur. The same criterion as the one which leads to Eq. 3, i.e. local Froude number of about 0.65, gives in terms of the integral variables a stratification condition

$$\frac{M(x)}{(Q(x)\ P_o H)^{1/2}} = 0.5 \qquad (14)$$

in which M(x) and Q(x) are the known solutions (Fig. 10) and $P_o = p_o\ L_D$. While plume restratification has been observed in Lee et al.'s and other experiments, the data is too inaccurate to allow a rigorous testing of Eq. 14. Even less is known about the evolution of the restratified intermediate field plume except for some qualitative observations which show strong lateral spreading much like the spreading of three-dimensional buoyant surface jets (22). For increasing depth H(x) the restratification tendency is even stronger (see Eq. 14). Field data from the FitzPatrick Station shows a rapidly restratifying plume due to a significant offshore slope.

4.2 Ambient Crossflow

Perpendicular alignment ("Coflowing" diffuser): The coflowing diffuser in which the nozzles are pointing into the same direction as the ambient crossflow, has qualitatively the same flow features as those under stagnant conditions. Its analysis - both for the slipstream and the complete

intermediate field - follows the same principles. The result for the bulk dilution (4, 30) is

$$S_a = \frac{1}{2} V + \frac{1}{2} \left(V^2 + \frac{2\, m_o H}{q_o^2}\right)^{1/2} \qquad (15)$$

in which $V = u_a H/q_o$ is simply the volume flux ratio between ambient and discharge flow. For $V = 0$, Eq. 15 reduces to the stagnant case, Eq. 8a. For strong crossflow, $S_a \approx V$, thus forced mixing, and the downstream slipstream contraction vanishes. Again, good agreement with experimental data has been found, which is indicated in Fig. 8 along with the stagnant case data. In a coastal current system whose velocity - but not flow direction - changes the bulk dilution is therefore variable according to Eq. (15). The performance of this diffuser alignment under tidal current reversals has been found (4, 18) to be very poor with intense temperature build-up zones occuring whenever the current opposes the nozzle direction.

River applications: The coflowing design is obviously the preferred design solution in riverine situations (28, 46). Here the effect of the lateral confinement of the shallow flow field becomes a crucial factor. The bulk dilution equation, Eq. 15, is applicable only if the diffuser does not extend across the entire river width. Under this condition, a local acceleration of the river flow is possible. The dilution capacity of a coflowing river diffuser is, ultimately, controlled by the available river flow Q_R. If the diffuser induced flow, $S_a Q_o$, is large, $S_a Q_o > Q_R$, then recirculation must take place, that is mixed water from the downstream region will return to the back entrainment region. The average dilution is then river controlled, $S_R = Q_R/Q_o$. This recirculation process has been observed in model studies related to the Browns Ferry plant (46). The river controlled

condition always applies when the diffuser extends fully across the river as has been simulated in numerous simple laboratory experiments.

Parallel alignment ("Tee" diffuser): Diffuser design in coastal environments is often carried out with the objective of providing sufficient offshore momentum to "push" the discharged effluent away from the shoreline. This objective is well achieved with the tee diffuser design under (near) stagnant conditions but it leads to significant reductions of initial dilutions under the influence of stronger currents. This adverse behavior is caused by the 90° mismatch between discharge momentum and crossflow momentum. Two effects are responsible: First, a local bending and overlapping of the individual discharge jets, and second, a recirculating eddy in the lee of the diffuser plume which is caused by rapid deflection of the entire discharge plume as the fully mixed plume blocks the ambient flow. Experimental data on the initial dilution - which is often difficult to determine because of large non-uniformities and plume break-up - have been correlated with the momentum ratio m_a/m_o. Lee et al. (31) have concluded an insignificant effect on dilution for small crossflow, $m_a/m_o < 0.1$, but rapid dilution reduction beyond that value. Analysis over a wider data range by Adams and Stolzenbach (5) lead to an empirical factor r_S which gives the dilution reduction relative to the stagnant value S, Eq. 8,

$$r_S = (1 + 5 \frac{m_a}{m_o})^{-1/2} \tag{16}$$

No analytical support for Eq. 16 is available nor is it easily derived due to the complicated flow geometry with recirculation zones. An equally empirical base is used in the analysis by Lee et al. (31) of the intermediate field plume trajectory of the tee diffuser. Their model computes the plume deflection on the basis of an entrainment force and drag force mechanism.

While that is standard practice in the modeling of three-dimensional jets in unbounded crossflow, it must remain rather tenuous in view of the strongly modified shallow ambient current whenever the plume blocks it. Possible plume restratification further complicates the situation. Using fitted drag coefficients, reasonable agreement with observed experimental trajectories was found, but different experimental conditions may necessitate coefficient adjustment. Finally, it should be mentioned that the offshore distance of a tee diffuser is also a critical parameter. A "starved" condition may arise when the diffuser is located too close to shore so that not sufficient ambient flow can penetrate to satisfy the downstream side entrainment demand in the lee of the plume. A plume shoreline attachment similar to that observed for buoyant surface jets (22) may result then. Again, restratification, possibly accelerated by an offshore slope, would somewhat abate that concern.

5. Staged Diffusers

The first diffuser designs which employed the staged diffuser concept were for the San Onofre Station (27) on the Pacific Coast and the Perry Station (3) on Lake Erie.

5.1. Stagnant Ambient

Structure of the flow field: Experimental observation (e.g. Fig. 12a) suggests an intermediate field plume structure which is made up of two zones: an acceleration zone along the entire diffuser length in which the diffuser momentum is gradually imparted to the ambient fluid, and, beyond the diffuser, a deceleration zone in which further lateral diffusion and bottom frictional dissipation takes place. In both zones, it is a side entrainment process which leads to plume dilution, unlike the unidirectional diffuser. A short three-dimensional zone, again of order of 5H to 10H length, exists at the upstream diffuser end before the unstable vertically mixed conditions are attained.

Analysis of the acceleration zone ("staged diffuser theory"):

Theoretical developments for the fully mixed acceleration zone, $0 \leq y \leq L_D$ - where $L_D \to \infty$ is possible in principle - have been given by Almquist and Stolzenbach (7, 8) and Lee (29), respectively. These references have used the entrainment approach with the assumption of self-similarity of lateral velocity and temperature profiles akin to the two-dimensional momentum jet. We will use here a different approach whose results seem to suggest that neither is self-similarity achieved for practical diffuser designs as the initial three-dimensional effects are of paramount importance nor is the analogy to the simple momentum jet entrainment process justified.

We first consider the asymptotic case of a true line source of vertically averaged momentum flux, m_o/H along the y-axis in two-dimensional space (or, equivalently, a plane source in three-dimensional space). Self-similarity is indeed possible (29) for this case as the only parameters to scale the lateral velocity profile u(x) at a given distance y are the constant flux m_o/H and y. However, what is the self-similar profile? Since at the centerline (x = 0) the diffuser is constantly imparting concentrated line momentum we expect infinitely high velocities there so that the analogy of the overall profile to the typical bell-shaped profile of simple jets is hardly appropriate. Therefore we use a superposition principle to estimate that velocity profile shape. Since the linear momentum profiles of individual sources of strength $m_o\, dy_1/H$, where dy_1 is a differential distance along $0 \leq y_1 \leq y$, are in the present situation simply additive, the total momentum profile can be obtained by simple integration from 0 to y. The main assumption made here is that lateral growth rate, $k = \frac{db}{dy}$, of the individual sources is equal to that for simple momentum jets in irrotational flow. This appears reasonable. For, consider the behavior of sources near the section of interest, $y_1 \pm y$: These

sources produce a locally intense vorticity field and perceive the already existing large scale, and hence weak, plume features as approximately irrotational. Using a Gaussian velocity profile, $e^{-\frac{x^2}{b^2}}$, where b is a measure of the local width, the momentum profile at y due to a differential source at y_1 is, by virtue of momentum conservation, $\frac{m_o}{H}\sqrt{\frac{2}{\pi}}\, e^{-\frac{2x^2}{b^2}}\frac{dy}{b}$, with $b = k(y-y_1)$. Integration along the diffuser and taking the square root gives then the composite velocity profile

$$u(x,y) = \left(\frac{m_o}{H}\right)^{1/2}\left(\sqrt{\frac{2}{\pi}}\frac{1}{k}\right)^{1/2}\int_0^1 e^{-\frac{2x^2}{k^2y^2(1-\eta)^2}}\frac{d\eta}{1-\eta}^{1/2} \qquad (17)$$

with $\eta = y_1/y$. The last factor in Eq. 17, simply denoted as $I^{1/2}(\frac{x}{ky})$, includes an exponential integral for which tabulated solutions (2) or numerical integration are adequate. The function $I^{1/2}$ gives the self-similar velocity distribution for a true line ($B \to 0$) staged diffuser and has highly concentrated core velocities (see Fig. 13).

In practice, the infinitely large velocites do not occur because the line diffuser assumptions do not hold (finite B) and, even more important, each source element has an initial three-dimensional zone until full momentum distribution over the entire water depth is achieved. Either of these two effects can be represented by a virtual source distance y_v. Thus, as far as surface conditions are concerned, we simply assume that only sources from 0 to $(y-y_v)$ influence the surface velocity profile at y. (Note: A more detailed, but lengthier approach would be to perform a superposition in three-dimensional but vertically limited space with a line source along x = 0,

$z = 0$. The resultant infinite series expression would presumably predict the actual vertically non-uniform conditions with higher influences near the bottom as has been observed experimentally (7)). The only difference in Eq. 17 is that the upper limit on the integral becomes $(1 - \frac{y_v}{y})$. The resulting non-dimensional velocity profiles, denoted by $I^{1/2}(\frac{x}{ky}; \frac{y_v}{y})$, are plotted in Fig. 13. Thus, the shape of the local velocity profile is critically dependent upon the three-dimensional zone effects. For increasing distance, $(\frac{y_v}{y})^{-1}$, the profiles undergo a constant evolution from an initial Gaussian shape $(\frac{y}{y_v} \gtrsim 1)$ to the final self-similar shape $(\frac{y}{y_v} \to \infty)$. The centerline velocity grows constantly in the process. A completely analogous superposition approach can be applied to the temperature flux, an equally conserved quantity. In general, the single source excess temperature profile may be given by $e^{-\frac{x^2}{\lambda_s^2 b^2}}$ where λ is a spreading factor between velocity and temperature profiles, usually $\lambda_s \approx 1.4$. If this is neglected ($\lambda_s = 1$), then the same non-dimensional profiles result for temperature, i.e. in Eq. 17 $u(x,y)$ is replaced by $\Delta T(x,y)$ and m_o by $j_o = \Delta T_o q_o$. This is assumed henceforth. (Note: If the excess spreading is not neglected then the temperature profiles are slightly depressed in the center and more spread out than the velocity profiles $I^{1/2}$. In particular, the centerline value for temperature would be $(\frac{1+\lambda_s^2}{2\lambda_s^2})^{1/2} I^{1/2}(0; \frac{y_v}{y})$, i.e. a small reduction by a factor of about 0.9.)

Using $k = 0.154$ (6, 41) as the appropriate spreading value for the single source Gaussian profiles, the centerline velocities and temperatures at the

diffuser end, $y = L_D$, are given by

$$u_c \left(\frac{m_o}{H}\right)^{-1/2} = \Delta T_c \left(\frac{j_o^2}{m_o H}\right)^{-1/2} = 2.28\ I^{1/2}(0; \frac{y_v}{L_D}) \qquad (18)$$

Eq. 18 is plotted in Fig. 14 together with experimental data. Since the staged diffuser profiles tend to become highly concentrated along the axis without a well defined plateau, it is difficult to find these local maxima in experiments. Almquist and Stolzenbach used a very fine measurement grid around the diffuser. Their observed surface temperature values are in good agreement with Eq. 18. Other studies (3, 44) determined the maximum surface temperature outside some exclusionary mixing zone. These "averaged" observations lie below the theoretical predictions. Yet regardless which observation criterion is chosen, all data, including some velocity observations, indicate a clear trend of increasing intensification as the relative diffuser length L_D/y_v increases. In all of these comparisons, y_v has been taken as 7.5H ($\approx \frac{1}{k^*} H$ where k* is likely some average between two- and three-dimensional jet spreading). This clear trend which is further supported by direct inspection of Almquist and Stolzenbach's data for $y_v < y < L$ exists despite the fact that all of the available experiments have some slope, $dH/dy > 0$, which would tend to counteract the intensification process (see Eq. 18).

The theory can also be used to define a volumetric (bulk) dilution as the ratio of laterally integrated discharge to diffuser discharge. Using the virtual source shift again, this bulk dilution is

$$S = 0.35 \frac{(m_o H)^{1/2}}{q_o} \frac{I^*(\frac{y_v}{y})}{1 - \frac{y_v}{y}} \qquad (19)$$

in which $I^*(\frac{y_v}{y}) = 2\int_0^\infty I^{1/2}(\frac{x}{ky};\ \frac{y_v}{y})d(\frac{x}{ky})$ and $(\sqrt{\frac{2}{\pi}}\ k)^{1/2} = 0.35$. Eq. 19 is also plotted in Fig. 14. Its asymptotic value at large distances ($\frac{y}{y_v} \to \infty$) is

$$S = 0.67\ \frac{(m_o H)^{1/2}}{q_o} = 0.67(\frac{\ell H}{a_o})^{1/2} \qquad (20)$$

and is practically approached for $y/y_v \gtrsim 3$ which is the range for most diffuser designs (L_D/y_v = 3 to 10). Interestingly, this value is considerably larger than the bulk dilutions predicted by the entrainment based theories which give a coefficient value of about 0.45 (8, 29). Unfortunately, no direct data are presently available to evaluate S.

In summary, it appears that the present theory which predicts an overall plume intensification within the staged diffuser acceleration zone is well supported by experimental evidence. It avoids the restrictions imposed by assuming overall similarity and, furthermore, overall entrainment characteristics similar to the simple momentum jet which has an entirely different internal force balance. Similar shortcomings in the use of constant entrainment hypothesis for boundary layer phenomena with variable force balances have been noted in connection with buoyant jet analysis (1, 24).

Complete intermediate field plume: Beyond the acceleration zone, $y > L_D$, the flow field gradually returns to a regular laterally diffusing plume flow. Bottom friction which had a negligible influence within the short acceleration zone becomes increasingly important. This is quite like the diffusion zone of the unidirectional diffuser, for which Eq.s 9 and 10 are the governing equations, except that $dP_e/dx = 0$ and x is replaced by y in the staged diffuser notation. In fact, the similar features at the end of the acceleration

zones for the two diffuser types are striking: The bulk dilutions S are of thesame order, vis. Eq.s 8 and 20, and so are the widths, about 0.5 L for the unidirectional and about $2\sqrt{2kL_D} = 0.44\ L_D$ for the staged diffuser. Thus, after a short adjustment zone, of order $5(2kL_D) = 1.5\ L_D$, beyond the diffuser the intermediate field flows for the two diffuser type are expected to be practically indistinguishable. Lee et al.'s theory for the diffusion zone of the unidirectional diffuser as summarized in Fig.s 10 and 11, should hold as well for the staged diffuser. This is demonstrated for example in Fig. 15 which compares predicted and observed excess isotherm areas.

Additional considerations: The question of nozzle orientation with repsect to the diffuser axis has received some attention. In some designs a slight alternating pattern (e.g. $\beta = \pm 25°$ for the San Onofre diffuser) and some upward angle ($\theta_o > 0°$) has been employed. In all of these, cases the same concentrated plume features persist, as individual jets become quickly deflected toward the plume axis (27), and the dilution is largely unchanged from the fully staged ($\beta = 0$, $\theta_o = 0$) diffuser. Suggestions that the y-momentum component should be taken only as $m_o \cos\beta \cos\theta_o$ seem unwarranted as the momentum becomes simply redirected into the y-direction. The extreme cases in this spectrum were probably the generic designs studied by the author (23) who considered variable nozzle orientations with $\theta_o = 45°$ and with $\beta(y) = \pm 90°(1 - \frac{y}{L_D})$ and $\beta(y) = \pm \cos^{-1}(\frac{y}{L_D})$, respectively. Thus, in both designs the first nozzles had, in fact, no y-momentum whatsoever! Still, the ultimate flow degenerated into a slender plume along the diffuser axis with intense deflection of the initial jets. Observed temperatures at the diffuser end are indicated in Fig. 14 with symbols ◇ and ⟡, respectively, without taking any reduction of the total momentum. This is but another, yet different, case of

a "locking into" of diffuser flow patterns despite seemingly contrary source conditions. Criteria for the actual control of these flow patterns will be developed in the next section.

The effect of variable depth, H(y), can be readily included in the above theoretical development. This has also been done by Lee (29) (using, however, the entrainment approach) who also discussed methods of discharge variations, $m_o(y)$, $j_o(y)$, to compensate for the increasing depth in case of an offshore slope. The position y of plume restratification in the downstream zone will be given by the same criterion, Eq. 14, (x replaced by y) that has been developed for the unidirectional diffuser. Again, increasing offshore depth will strongly promote restratifiction. Finally, we can use, Eq. 14, evaluated at $y = L_D$ together with the bulk flow expression, $S\, q_o\, L_D$, where S is from Eq. 20, to find a criterion of applicability for the fully mixed assumption within the acceleration zone. This criterion is

$$\frac{m_o}{p_o^{2/3} H} \geq 0.52 \qquad (21)$$

In a way, this equation might be considered as an alternative near-field stability criterion since the two-dimensional channel assumptions which lead to Eq. 2 are hardly justified for a staged diffuser. Data analysis by Almquist and Stolzenbach (8) seem to suggest an even higher critical value, (possibly up to 2), but that conclusion needs further testing as the only stratified observations come from a distorted scale model study with strong offshore slope (27).

5.2. Ambient Crossflow

Perpendicular alignment: This is the only alignment solution of interest in normal coastal situations as it combines good offshore transport of the diffuser plume during stagnant conditions with a good capture of longshore

current flow from either direction. Since the diffuser momentum and ambient momentum act at a right angle to each other, it is reasonable to propose a vector addition of the two resulting bulk mixing effects, so that the total bulk dilution becomes by virtue of Eq. 20

$$S_a = 0.67 \frac{(m_o H)^{1/2}}{q_o} [1 + 2.23 \frac{V^2 q_o^2}{m_o H}]^{1/2} \qquad (22)$$

where the square bracket expression represents the current induced mixing amplification. The factor $V^2 q_o^2 (m_o H)^{-1}$ can also be written as the momentum ratio m_a/m_o. Eq. 22 is compared in Fig. 16 with available data from several experiments. Brocard (11) has derived a somewhat different expression based upon an extension of an entrainment based staged diffuser model. However, the difference appears to be less than the considerable scatter in the experimental data which reflects to a large extent the different averaging techniques employed in these studies.

Brocard et al (12) have developed a model for the complete trajectory of a staged diffuser plume in crossflow, including the effect of restratification. Their model showed good agreement with available experimental data (12, 38), but includes several fitting coefficients and some of the same reservations may be raised that apply to Lee et al.'s (31) trajectory model for unidirectional diffuser plumes.

6. Alternating Diffusers

The alternating diffuser concept has been a traditional design solution for buoyancy dominated sewage outfalls into the ocean. Its first applications for power plant discharges were the Shoreham Station (18) and the Northport Station (17) diffusers, both on Long Island Sound.

6.1 Stagnant Ambient

Two-dimensional channel analysis: The dilution characteristics of a properly designed alternating diffuser are controlled by the restratification of the intermediate field flow just outside the unstable near field zone. Thus the bulk dilution is influenced by buoyancy effects rather than pure momentum effects as is the case for unidirectional and staged diffusers. We first explore this mechanism in the simpler two-dimensional channel framework (Fig. 3). For the alternating diffuser with nozzle angle θ_o(A) - or in the limit, the vertical discharge, $\theta_o = 90°$ - a symmetric flow field results. Detailed experimental data (21, 23) show an unstable near field consisting of a recirculating cell of approximate length 2.5H which is then followed by a stratified counterflow in the intermediate field (Fig. 17). The primary role of the near field is the dissipation of the excess momentum of the discharge. Hence the momentum flux m_o looses its significance as a dynamic parameter. The bulk mixing, i.e. the ratio of ambient entrained flow to discharge flow, $S = \frac{2q_1}{q_o}$, is rather determined by the stratified flow dynamics of the intermediate field. That is, given the buoyancy flux p_o as the remaining active element, what strength q_1 of the counterflow system is maintained in steady state against the opposing forces of bottom friction τ_b, interfacial friction τ_i and convective accelerations at the control points C? The answer is given by the classical Schijf and Schonfeld (42) stratified flow equations solved for equal counterflow (23, 24) and resulting in

$$S = (2F_H)^{2/3} \frac{p_o^{1/3} H}{q_o} \qquad (23)$$

in which F_H = densimetric Froude number of the stratified counterflow and a

function of friction and relative channel length, $F_H = f(\Phi_c = \lambda \frac{L_c}{H}, \frac{\lambda_i}{\lambda})$, in which $L_c = L - 2.5H$ and λ_i = an interfacial friction parameter. The maximum value of F_H occurs for zero counterflow length, $\Phi_c = 0$, and is given as a pure inertial control, $F_H = 1/4$. Increasing Φ_c decreases F_H and hence leads to reduced dilutions S. Eq. 23, in normalized form and assuming $\lambda_i/\lambda = 0.5$, is plotted in Fig. 18 along with experimental data obtained from a channel within a large surrounding basin (23, 24). A clear sensitivity to the intermediate field effects is evident.

Three-dimensional alternating diffuser with stratified flow field: If annihilation of excess momentum within the near field and a buoyancy driven exchange flow is the dilution mechanism for an alternating diffuser within bounding channel walls, can a similar mechanism be achieved in the three-dimensional unstable case with finite diffuser length LD? An analysis (4) is given below which demonstrates that a special horizontal momentum distribution $\pm \vec{m}_o^*(y) \cos \theta_o(A)$, i.e. a variable nozzle alternating orientation $\pm \beta^*(y)$, must be maintained to insure stratified flow in the intermediate field. If the actual nozzle distribution deviates significantly from that special one, then instabilities which originate within the unstable near field become amplified and lead to vertically mixed horizontal circulation cells within each quadrant of the xy plane.

Consider the diffuser line with the surrounding unstable near field zone (total width ≃ 5H) shown in Fig. 19. Under stably stratified flow conditions in the intermediate field we expect a lower layer flow toward the diffuser line as indicated by the streamlines. An approximately equal, but reversed, flow pattern should result for the flowaway of mixed water within the surface layer. Assuming, in steady state, an approximately constant interface location at half depth and, as has been done above, neglecting friction in the

diffuser vicinity (scale length L_D) allows a simple two-dimensional inviscid analysis. Taking uniform dilution along the diffuser line (because of uniform buoyancy flux), the total sink strength, μ_o, per unit depth and length is

$$\mu_o = 2Sq_o/H \tag{24}$$

Using complex notation $\xi = x + iy$, the potential due to a differential sink at ζ is $dW = -\frac{\mu_o i\, d\zeta}{2\pi} \log(\xi - \zeta)$ where $-i\frac{L_D}{2} \leq \zeta \leq i\frac{L_D}{2}$. Integration over the diffuser length gives

$$W = \frac{\mu_o}{2\pi}\left\{i \log \frac{(\zeta + i\,L_D/2)^{\zeta+iL_D/2}}{(\zeta - i\,L_D/2)^{\zeta-iL_D/2}} + iL_D\right\} \tag{25}$$

The complex layer-averaged flow field in the ξ plane is after differentiation

$$\tilde{u} - i\tilde{v} = \frac{\mu_o}{\pi}\left[\tan^{-i\frac{2\xi}{L_D}} - \frac{\pi}{2}\right] \tag{26}$$

and evaluated at the diffuser line

$$\tilde{u}_D - i\tilde{v}_D = \frac{\mu_o}{\pi}\left[\tan^{-1}\frac{2\,iy}{L_D} - \frac{\pi}{2}\right] \tag{27}$$

This gives the angle $\beta^*(y)$ under which the flow approaches the diffuser line, $\cot\beta^* = \tilde{v}_D/\tilde{u}_D$, or

$$\beta^*(y) = \pm\cot^{-1}\left(\frac{1}{\pi}\log\frac{1 + 2y/L_D}{1 - 2y/L_D}\right) \tag{28}$$

The streamlines ψ corresponding to Eq. 25 and the intersecting angle β^* are plotted in Fig. 19.

The object of alternating diffuser control is now to orient the horizontal component of the discharge momentum $\vec{m}_o^*(y) \cos \theta_o(A)$ so as to oppose the momentum flux which is carried by the incoming entrainment flow. The vertical angle $\theta_o(A)$ must be kept below a certain maximum in order to have sufficient opposing momentum. For any streamtube of width $\Delta\psi = u_D H/2$ the incoming momentum is $\tilde{u}_D^2 H (2 \sin \beta^*)^{-1}$ while the opposing momentum is $m_o \cos \theta_o(A)(2 \sin \beta^*)^{-1}$ in which m_o = total diffuser momentum flux (one half to each side). Thus, by virtue of Eq. 24

$$\cos \theta_o(A) \geq \frac{s^2 q_o^2}{m_o H} \tag{29}$$

independent of y, and using Eq. 23

$$\theta_o(A) \leq \theta_o^{max}(A) = \cos^{-1}[(2 F_H)^{4/3} \frac{p_o^{2/3} H}{m_o}] \tag{30}$$

Eq. 30 is evaluated, taking the most extreme condition, a very short diffuser, $\phi_c \to 0$, $F_H = 1/4$, that is operating just in the unstable domain, $m_o/(p_o^{2/3} H) = 0.54$ (see Eq. 2 for zero net horizontal momentum). The result is $\theta_o^{max}(A) \simeq 45°$. Larger angles are possible for more unstable conditions. Thus, an alternating diffuser with unstable near field should have a variable nozzle distribution $\beta^*(y)$ given by Eq. 28 and a vertical angle less than $\theta_o^{max}(A)$ in order to insure a controlled stably stratified flow in the surrounding intermediate field. No diffuser control is possible for vertically discharging ($\theta_o = 90°$) unstable diffusers. No diffuser control is necessary for stable near field diffusers nor do the nozzle angles, $\beta(y)$ or $\theta_o(A)$, matter much.

These theoretical proposals have been tested and verified (23) in a series of experiments conducted with an alternating half diffuser (x,+y half plane) with the x-axis along the basin wall. Fig. 20a gives a photographic sequence for an unsteady dye release into the steady state flow field, $\beta^*(y)$, $\theta_o(A) = 0°$: (i) The dye pulse enters through nozzles at the diffuser end and center, respectively, showing spreading in all directions. (ii) The dye pulse now occupies the entire diffuser length and has spread more. (iii) Shortly, after the dye has been stopped, the entire surface area (20H x 20H is shown, with the diffuser half length $L_D/2H = 12$) is occupied by dyed, but diluted, water giving an indication of the stratified flow structure. The temperature field for a similar experiment, $\beta^*(y)$, $\theta_o(A) = 45°$, is given in Fig. 21a. The surface isotherms show spreading in all directions from the diffuser line and vertical profiles at four points within the intermediate field demonstrate the stratified structure. The near field in these cases is strongly unstable (vis. Eq. 2) and represents the region where the excess discharge momentum is dissipated while opposing the entrainment momentum.

Having established the possibility of three-dimensional stratified intermediate field flow it remains to relate its bulk dilution to that which has been derived under the channel approximation, Eq. 23. This may be done on the basis of equivalent frictional effects in the intermediate field. For while friction has negligible effects on the flow dynamics (i.e. the shape of the streamlines in Fig. 19) it ultimately determines the magnitude of the flow (i.e. the value of the streamfunction). The total head loss due to bottom friction in the channel model is approximately

$$h_{f2\text{-}D} = \lambda \frac{L}{H} \frac{1}{g} \left(\frac{q_o S}{H}\right)^2 \tag{31}$$

assuming again a lower layer thickness H/2. The total head loss in the three-

dimensional case for a streamtube along the x-axis is given by the integral

$$h_{f3-D} = \int_0^\infty \lambda \frac{1}{H} \frac{1}{g} \tilde{u}^2(x,0)dx \tag{32}$$

Substituting Eq. 26, gives

$$h_{f3-D} = \lambda \frac{L_D}{2H} \frac{1}{g} \left(\frac{q_o S}{H}\right)^2 \left[\left(\frac{2}{\pi}\right)^2 \int_0^\infty (\tan^{-1}\eta - \frac{\pi}{2})^2 d\eta\right] \tag{33}$$

in which $\eta = 2x/L_D$. The value of the definite integral is π ℓn 2 (2). Similar relationships could be constructed for the head losses due to interfacial friction. Thus, comparing Eq.s 31 and 33, equivalent kinematic (dilution) and dynamic (head loss) effects in the intermediate field requires

$$L = 0.884\left(\frac{L_D}{2}\right) \tag{34}$$

For practical purposes, given the approximations involved, the total channel length should be of order diffuser length, a reasonable result, or in terms of the frictional parameters

$$\Phi_c \simeq \frac{1}{2} \Phi \tag{35}$$

Data from three-dimensional diffuser experiments with nozzle control are also included in the normalized dilution diagram (Fig. 18). The dilution S is here evaluated at the edge of a near field mixing zone of area $A_m = 5HL_D$ around the diffuser line. The agreement is good, supporting the equivalency argument.

Additional temperature reduction in the intermediate stratified flow field: In the preceding stratified flow analyses a stable interface with no diffusion or entrainment has been assumed. Observations in the laboratory suggest, however, that additional slow mixing is taking place in the interme-

diate field which leads to further surface temperature reductions beyond the near field value. Data from basin experiments (23) is shown in Fig. 22 giving the non-dimensional temperature rise, $\Delta TS/\Delta T_o$, as a function of scaled isotherm area, A/A_m. The indicated experimental trend may be used for estimation purposes, but caution must be exercised as the experimental data, for large areas relative to the available basin size are affected by unavoidable transient effects. Furthermore, surface heat loss may also play a role in the temperature decrease. In summary, the alternating diffuser flow field experiences a smooth transition from the intermediate field to the far field processes which cause ultimate diffusion and dissipation of the excess heat.

Deviations from the controlled nozzle orientation $\beta^*(y)$: If the diffuser momentum input deviates significantly from the controlled condition, then stratified flow breakdown occurs and fully mixed horizontal circulations are generated. The sense of these circulations depends on the sense of the deviation. Consider first a deviation $\beta(y) > \beta^*(y)$, or in the limit $\beta = \pm 90°$, the "traditional" alternating diffuser design. Here, the diffuser ends have no momentum to oppose the entrainment momentum flux which approaches along the $\pm$ y-axis. Hence, an instability arises at the ends and a current is set up which sweeps in to meet the entrainment demand of the jets in the diffuser center. After mixing and transfer of some of the discharge momentum, this current then leaves as a vertically fully mixed flow perpendicular to the diffuser along the $\pm$ x-axis. This sequence is shown in Fig. 20b: Photographs (i) to (iii) show the fate of the dye pulse emitted from the diffuser ($\beta = \pm 90°$, $\theta_o = 0°$(A)) into the steady state flow field. The dashed lines have been drawn in to suggest the boundaries of the contracting plume motions. A recirculation cell is generated in each quadrant of the xy plane. Despite the geometry difference, this flow structure somewhat resembles that of the unidirectional diffusers: the "back entrainment" flow is simply

squeezed into a narrow zone between the y-axis (x = 0) and the line at which complete vertical momentum transfer has been achieved (x = 5 to 10H). In fact, just as the unidirectional diffuser has an analogy in three-dimensional aerodynamics, i.e. the propeller, there exists a three-dimensional analogy here as well: multiple propulsion jets issuing from a bluff body, such as at the bottom of a rocket or VTOL aircraft. For example, Baines and Keffer (10) observed similar contracting motions for a 17 nozzle propulsion assembly. No simple bulk dilution theories are available for analysis as the irrotational assumption is surely not justified and significant losses occur within this complex motion. A similar lack of control is also indicated by a purely vertical, $\theta_o = 90°$, diffuser with unstable near field. This is shown by the temperature velocity arrows given in Fig. 21b: The vertically mixed flow (profiles 2 and 4) along the $\pm$ x-axes is evident. The small stratification elsewhere (profiles 1 and 3) is merely a gradual secondary restratification effect in the intermediate field. Thus, even though the initial discharge carries no horizontal momentum whatsoever, the shallow water instabilities ultimately cause a re-direction of that momentum and give rise to significant horizontal circulations! We must emphasize again, that this does not occur for stable near field diffusers: Observations by Liseth (33) and the author (23) only show a slight inward bending of the rising buoyant jets at the diffuser end, but otherwise a stably stratified flow field.

The second deviation of interest is $\beta(y) < \beta^*(y)$, or in the limit $\beta \to 0°$, the staged diffuser, or rather a "diffuser doublet" issuing into both $\pm$ y directions. Here, the maximum momentum mismatch exists in the diffuser center ($y \approx 0$) where the instabilities start and then degenerate into mean currents toward the diffuser end. Data for diffuser motions which meet $\beta(y) < \beta^*(y)$, but are not fully staged, have been mentioned earlier (vis. Fig. 14). Again, the diffuser induced motions experience a momentum re-direction - this time

into the $\pm$ y-direction - which is initially triggered by the instabilities.

A convenient summary of these generic diffuser characteristics is provided in Fig. 23 for the first quadrant of the flow field. The figure illustrates that, within a continuous spectrum of shallow water diffuser designs, there are only three fundamental flow patterns: the "unidirectional" pattern with flow away perpendicular to the diffuser, the "staged" pattern with flow away parallel to the diffuser and, in between, the controlled "alternating" pattern with stratified flow away into all directions. Accumulated evidence has shown that the first two are clearly "lock in" patterns, that is, easily generated and readily maintained horizontal circulations. To what extent, the alternating diffuser pattern is a stable one that is resilient to some deviations from the optimal $\beta^*(y)$ or to dynamic perturbations is an obvious concern. The author's experiments which involved variable orientations and clearly had imperfections in the nozzle orientation (e.g. only a few nozzles) demonstrated that the stratified flow field was persistent over long time and even in presence of weak ambient currents. No breakdown motions occured if $\beta^*(y)$ was reasonably provided. Still, further refined study seems needed in view of some of the approximations which lead to the definition of $\beta^*(y)$ in the first place and to define permissible deviations from the optimal distribution.

6.2 Ambient Crossflow

Perpendicular alignment: As for the staged diffuser this is the preferred alignment in the open coastal environment. Again, a vector addition of the two asymptotic dilution effects is most reasonable, giving a crossflow dilution S_a

$$S_a = (S^2 + V^2)^{1/2} \tag{36}$$

in which S is given by the stagnant value, Eq. 23. Available data from both a

channel model and the three-dimensional diffuser with nozzle control are compared to Eq. 36 in Fig. 24. Even though the predictions are slightly high, the additive effect assumed in Eq. 36 is borne out by the data. Incidently, this is in marked contrast to the behavior of strongly buoyant diffusers (with negligible discharge momentum) in crossflow as observed by Roberts (40) who found surface dilutions typically less than the minimum asymptotic value V. This is another documentation of the strongly modifying effect of an unstable diffuser near field (20). The unstable near field, of course, does not preclude restratification at some distance downstream from the diffuser which has, in fact, been observed for most of the three-dimensional cases reported on Fig. 24.

Parallel alignment: An alignment parallel to the current may be necessitated by special siting constraints, e.g. navigational requirements at the Cape Cod Canal Plant (16). The dilution performance is obviously reduced relative to the perpendicular alignment, a reduction of about 20% being typical (23).

7. Aspects of Diffuser Design

7.1 General Design Considerations

Diffuser design practice consists of finding an acceptable tradeoff between the economic costs and the environmental impacts of a diffuser installation. The major cost component is the construction cost of the underground pipeline, comprising the actual diffuser and its feeder line from the shore. For large installations construction costs (e.g. tunneling) may exceed $10,000 per foot so that for mile long pipelines total costs can easily surpass $100 million. This represents a large investment both in absolute terms and relative to the total plant cost. Lifetime operational costs, due to energy losses in long pipelines or for high discharge velocities, are an additional element.

We may divide the environmental impacts into those related to the induced temperature field and those related to the induced velocity field. The temperature factor which has traditionally received most attention, both by biologists and regulatory personnel and, in turn, by design engineers, is the near field temperature rise. This excess temperature value, ΔT_{max}, - for regulatory evaluation and enforcement reasons - is mostly defined at the water surface and may include a small exclusion zone ("near field mixing zone"). Even though a ΔT_{max} constraint is still the major target value in design practice much more attention has been given in recent years to a more holistic and ecologically meaningful evaluation of the temperature impact. Temperature parameters, such as larger scale surface area - temperature rise relationships, volume - temperature rise relationships, temperature rise - exposure time relationships, temperature rises at the bottom (benthic organisms), temperature rises at the shoreline (littoral organisms), recirculation effects into the power plant intake etc., are often of equal importance and may affect not only diffuser design but site selection as a whole.

On the other hand, the engineering community has given very little consideration to the diffuser induced velocity field and the resulting modification of the ambient coastal hydrography. The potential for this modification clearly exists for large scale installations (see Table 1) and depends on diffuser type. The major consequences relate to the altered transport characteristics of the coastal zone, as regards transport of passive biological species and, more importantly, of sediment. A more direct impact on navigation is another possibility. The effect on sediment transport, if any, is naturally strongly dependent upon type of substrate, offshore bathymetry and natural transport rates. We may visualize two specific mechanisms by which diffuser operation may disrupt the natural transport regime. (i) Littoral, wave induced sediment transport appears to occur in about equal portions with-

in the actual breaker zone and within the shelf zone further offshore (Grant, personal communication). The transport distribution within the shelf zone itself depends strongly upon bathymetry. If the shelf is weakly sloping (typical on U.S. East or Gulf coasts) then significant transport can occur to large offshore distances until sufficient water depth has been reached. If the shelf is strongly sloping (as on the U.S. West coast), then the transport rate drops off rapidly with offshore distance. Thus, the likelihood of diffuser interaction with this natural transport mode, is related to the diffuser location relative to the active shelf zone. If the diffuser is located outside that zone (e.g. West coast diffusers) then very little affect is likely. On the other hand, if a weak slope dictates a diffuser location somewhere within the active shelf zone, then strong interaction is likely. The degree of interaction depends upon diffuser type. For example, a diffuser with strong offshore momentum, such as the staged type, may effectively capture a significant portion of the littoral sand transport and push it offshore, thereby possibly causing offshore accretion and downshore erosion. Wave induced bottom shear velocities on the shelf during a major East coast storm may be of the order of 5 to 10 cm/s (0.15 to 0.3 ft/s) (Grant, personal communication). This leads to strong sediment transport rates as ascertained by indirect observations which compare shelf conditions before and after such storms. Diffusers which produce strong horizontal circulations can readily set up local shear velocities of equal magnitude. Thus, the possibility of local erosion exists in addition to the offshore diversion of littoral transport. (ii) A second mechanism by which diffuser operation can even affect the near shore transport within the breaker zone has been mentioned by Raichlen (personal communication). The wave-current interaction with the net horizontal circulation produced by certain diffuser types will, in principle, lead to wave refraction and focusing. This, in turn, leads to imbalances in the wave energy density along the shoreline. For a diffuser with strong off-

shore momentum, the possibility exists for local sand accretion effects at the shoreline and the gradual formation of a tombolo.

Certainly, much additional quantitative work together with detailed field observations on operating diffusers is needed to assess the long term impact (say, over half a century of operation) on the coastal morphology. However, the potential for some impact is likely, at least for those diffuser types with strong net circulations. This should not be surprising in view of the fact that some of these diffusers are large engineering structures which - after mixing - produce flows of the order of very large rivers (31) entering the coastal zone. Thus, the long term sedimentary activity should not be unlike that at some river mouths or tidal inlets or around some engineering structures, such as artificial harbors, jetties or offshore islands.

Despite the aforementioned variety of environmental impacts, we will assume for purposes of the following design comparison that the major constraint is given by a near field temperautre rise ΔT_{max}. Also, in most cases, this assumption is adequate for the screening of initial designs. Given the predictions for induced temperature rises which have been summarized in the earlier sections, we can therefore derive equations for the length requirements L_D for the three diffuser types. Given a power plant with discharge Q_o, temperature rise ΔT_o, therefore $g'_o = \frac{\Delta\rho_o}{\rho_a} g = \beta_e \Delta T_o g$ where β_e = coefficient of thermal expansion, discharge velocity U_o and ambient depth H, these length requirements are:

Unidirectional diffuser (from Eq. 8):

$$L_D = \left(\frac{\Delta T_o}{\Delta T_{max}}\right)^2 2 \frac{Q_o}{H U_o} \tag{36}$$

Staged diffuser (from Eq. 18):

$$L_D = \left(\frac{\Delta T_o}{\Delta T_{max}}\right)^2 (2.28\ I^{1/2})^2 \frac{Q_o}{H\ U_o} \tag{37}$$

in which $I^{1/2}$ is plotted in Fig. 13 and is a weak function of diffuser length with typical values between 1.0 and 1.5.

Alternating diffuser (from Eq. 23):

$$L_D = \left(\frac{\Delta T_o}{\Delta T_{max}}\right)^{3/2} \frac{1}{2\ F_H} \frac{Q_o}{H^{3/2}\ g'^{1/2}_o} \tag{38}$$

in which $(2F_H)^{2/3}$ is plotted in Fig. 18 as a function of the friction parameter Φ with typical values between 0.45 to 0.55; i.e. F_H between 0.15 and 0.20.

The qualitative difference in the peak temperature value ΔT_{max} implied in these design equations must be kept in mind here. ΔT_{max} represents a slip stream temperature plateau for the unidirectional diffuser, a concentrated temperature maximum above the diffuser line (predominantly at its end) for the staged diffuser and a mixing zone of total width ≈ 5H surrounding the alternating diffuser line. Furthermore, the design equations are limited to the worst case assumption of stagnant (or very weak) ambient velocities. These differences will be further illuminated in the following design example.

7.2 A Design Comparison

We illustrate for a typical large diffuser installations the differences in near field mixing related length requirements and in various environmental impact measures. More detailed sensitivity studies which explore the parameter variability indicated by Eq.s 36 to 38 but limit themselves to the singular aspect of near field mixing have been given by Adams and Stolzenbach (5) and Paddock and Ditmars (36).

A 2000 MW nuclear power plant with the characteristics given in Table 1 is assumed together with a coastal bathymetry with an initially sloping bottom and a uniform shelf depth of 10m (33 ft) reached after a distance of 500m (1640 ft). These conditions (see Fig. 25) may be typical for U.S. East or Gulf coasts or the Great Lakes. The coastal currents have a maximum strength of 0.3 m/s (1 ft/s) allowing for both cases of reversing and one-directional currents. A maximum allowable near field temperature rise, ΔT_{max}, of 1.5°C (2.7°C) governs the design and corresponds to a diluton of 8.

The design parameters and environmental impact characteristics of the three diffuser types are summarized in Table 2 and Fig. 25. Temperature impacts are indicated by the surface isotherm areas associated with ΔT_{max} and 0.5 ΔT_{max}, respectively. Velocity impacts are indicated by the maximum induced velocities.

The unidirectional diffuser has usually the least length requirement. Its alignment is dependent upon the nature of the ambient current regime. For non-reversing currents (also in rivers) the coflowing alignment is the obvious one. For reversing, but weak, currents an offshore orientation (tee diffuser) is possible. In strong reversing current systems, however, any unidirectional design seems undesirable. Also when a tee diffuser design is chosen it may be appropriate to move the diffuser location an additional distance (200m in our example) offshore to provide sufficient space for the back entrainment flow and prevent a "starved" plume condition.

The staged diffuser has intermediate length requirements. It is interesting to note that the large scale mixing capacity, as indicated by the area of the $\frac{1}{2}\ \Delta T_{max}$ isotherm, is similar to that for the unidirectional diffuser which has the same horizontal momentum input. Under cross-currents the diffuser performs well and independently of current direction.

The alternating diffuser generally requires the longest diffuser section. Also the extent of the $\frac{1}{2}\,\Delta T_{max}$ isotherm is somewhat larger because of the lack of an intensive mixing action in the intermediate field. Using the perpendicular alignment as the obvious choice, the mixing characteristics in a reversing current system are excellent.

These length requirements for the three diffuser types have to be contrasted with the fundamental differences in their temperature and flow fields as summarized in Table 2 with various impact measures and qualitative comments. Finally, it must be stressed again that not the diffuser length, L_D, alone but rather the total pipe length, TPL, to shore is the major cost parameter. If the feeder pipe is long, due to local bathymetry or shoreline impact constraints, then the relative differences in total pipe length can become minor. In our present example, if the staged diffuser is taken as the average (TPL = 1250m), then the relative deviations are $\pm$ 40% for the alternating and unidirectional designs and, thus, reasonably modest when compared to the differences in diffuser length alone.

8. Conclusions

A summary has been given of the fluid mechanical characteristics - as derived from theory and experimental observation - of submerged multiport diffusers used for the disposal of cooling water from thermal power plants. First and foremost among these characteristics is the near field instability produced by such thermal diffusers in typical receiving water conditions. Rather than forming a distinct buoyant plume as is the case for sewage diffusers, the high discharge momentum of thermal diffusers leads to a flow breakdown with local recirculation zones and full vertical mixing. The flow and temperature fields at larger distances, in the interemediate field, are then critically dependent upon how the discharge momentum is introduced into the ambient fluid layer. Out of a spectrum of possible diffuser designs three

major types have evolved. The unidirectional and the staged diffusers are designs which result in concentrated vertically mixed intermediate field motions. The alternating diffuser with nozzle control, on the other hand, generates a stratified flow field outside the unstable near field. Predictive techniques for these basic types have been summarized, both for the stagnant ambient case and for the additional influence of a current system. These techniques, together with an appreciation of the fundamentals of shallow water diffuser behavior, should be useful for the design engineer in tailoring a diffuser design to the specific needs of a heat disposal situation.

Numerous problem areas await further clarification. Some of these have been mentioned in the preceding sections. Perhaps most important is detailed operational data on field diffuser installations, not only to verify the predictive capabilities developed thus far but also to define the actual environmental impacts of these major engineering structures. For example, could such data indicate that the induced near field temperature rise which was the prime concern in the past might in fact be far less critical in an overall evironmental context than modification of the coastal hydrography and sediment transport patterns? Finally, considerable advances have been made in recent years in applying computer based higher order turbulence models to reasonably complex hydraulic problems. Yet no successful application to the shallow water diffuser case has been reported and the momentum boundary condition at the diffuser line clearly poses a special difficulty. Thus, the development of a general diffuser theory, valid for arbitrary diffuser and receiving water geometries, remains a challenge for the future.

Acknowledgements

During several years of research on diffusers, the writer has had the benefit of a close cooperation with students and colleagues at M.I.T. and Cornell University. Their ideas and contributions are, in part, reflected in

this review. Above all, special thanks are due to Prof. Donald R. F.Harleman. It was he who first suggested this problem area as a thesis topic and who, in the years since, has been a constant source of scientific advice, criticism and encouragement alike. Discussions with Drs. A. Dalrymple, W. Grant and F. Raichlen on the potential interaction of diffusers with coastal sediment transport are gratefully acknowledged.

References

1. Abraham, G., 1965, Entrainment principle and its restriction to solve jet problems, J. Hydraul. Res., I.A.H.R., 31, 1-23.

2. Abramowitz, M. and Stegun, I. A., 1964, Handbook of Mathematical Functions, National Bureau of Standards, Applied Mathematics Series 55.

3. Acres American Inc., 1974, Perry Nuclear Power Plant; Thermal hydraulic model study of cooling water discharge, Tech. Rep., Buffalo, New York.

4. Adams, E. E., 1972, Submerged multiport diffusers in shallow water with current, M.S. Thesis, Dept. of Civil Engineering, Massachusetts Institute of Technology.

5. Adams, E. E. and Stolzenbach, K. D., 1977, Comparison of alternative diffuser designs for the discharge of heated water into shallow receiving water, Proc. Conf. on Waste Heat Management and Utilization, Vol. I., p. 2c-171, Miami Beach, Florida.

6. Albertson, M. L., Dai, Y. B., Jensen, R. A. and Rouse, H. 1950, "Diffusion of submerged jets", Trans. A.S.C.E., 115, 639-664.

7. Almquist, C. W. and Stolzenbach, K. D., 1976, Staged diffusers in shallow water, R. M. Parsons Lab. for Water Resources and Hydrodynamics, Tech. Rep. 213, Massachusetts Institute of Technology.

8. Almquist, C. W. and Stolzenbach, K. D., 1980, Staged multiport diffusers, J. Hydraul. Div., Proc. ASCE, Vol. 106, HY2.

9. Argue, J. R. and Sayre, W. W., 1973, The mixing characteristics of submerged multiport diffusers for heated effluents in open channel flow, Iowa Institute for Hydraulic Research, Tech. Rep. 147, Iowa City, Iowa.

10. Baines, W. D. and Keffer, J. F., 1974, Entrainment by a multiple source turbulent jet, Advances in Geophysics, Vol. 18B, p. 289, Academic Press.

11. Brocard, D. N., 1980, Discusson of "Staged multiport diffusers" by Almquist, C. W. and Stolzenbach, K. D., J. Hydraul. Div., Proc. ASCE, Vol. 106, HY10.

12. Brocard, D. N., Beauchamp, C. H. and Hsu, S. K., 1979, Analytical predictions of staged diffuser performance: Palisades Nuclear Generating Station, Alden Research Laboratory, Tech. Rep. 84-79.

13. Buhler, J., 1974, Model studies on multiport outfalls in unstratified stagnant or flowing receiving water, Ph.D. Thesis, Dept. of Civil Engineering, University of California, Berkeley, Calif.

14. Cederwall, K., 1971, Buoyant slot jets into stagnant or flowing environments, W. M. Keck Lab. for Water Resources and Hydraulics, Tech. Rep. KH-R-25, California Institute of Technology.

15. Harleman, D. R. F., 1960, Stratified Flow, in Handbook of Fluid Dynamics (V. L. Streeter, Ed.), McGraw Hill Book Co.

16. Harleman, D. R. F., Jirka, G. H., Adams, E. E. and Watanabe, M., 1971, Investigation of a submerged slotted pipe diffuser for condenser water discharge from the Cape Cod Canal Plant, R. M. Parsons Lab. for Water Resources and Hydrodynamics, Tech. Rep. 141, Massachusetts Institute of Technology.

17. Harleman, D. R. F., Jirka, G. H. and Evans, D. H., 1973, Experimental Investigation of submerged multiport diffusers for condenser water discharge with application to the Northport Electric Generating Station, R. M. Parsons Lab. for Water Resources and Hydrodynamics, Tech. Rep. 165, Massachusetts Institute of Technology.

18. Harleman, D. R. F., Jirka, G. H. and Stolzenbach, K. D., 1971, A study of submerged multiport diffusers for condenser water discharge with application to the Shoreham Nuclear Power Station, R. M. Parsons Lab. for Water Resources and Hydrodynamics, Tech. Rep. 139, Massachusetts Institute of Technology.

19. Jain, S. C. et al., 1971, Model studies and design of thermal outfall structures Quad-Cities Nuclear Plant, Iowa Institute of Hydraulic Research, Tech. Rep. 135, Iowa City, Iowa.

20. Jirka, G. H., 1979, Discussion of "Line plume and ocean outfall dispersion" by P. J. W. Roberts, J. Hydraul. Div., Proc. ASCE, HY12.

21. Jirka, G. H., to appear, Turbulent buoyant jets in shallow fluid, Ch. 4 of Turbulent Buoyant Jets and Plumes, W. Rodi, Ed., Pergamon Press.

22. Jirka, G. H., Adams, E. E. and Stolzenbach, K. D., 1981, "Properties of buoyant surface jets", J. Hydraul. Div., Proc. ASCE, Vol. 107.

23. Jirka, G. H. and Harleman, D. R. F., 1973, "The mechanics of submerged multiport diffusers for buoyant discharges in shallow water", Ralph M. Parsons Laboratory for Water Resources and Hydrodynamics, Tech. Rep. 169, Massachusetts Institute of Technology.

24. Jirka, G. H. and Harleman, D. R. F., 1979, Stability and mixing of vertical plane buoyant jet in confined depth, J. of Fluid Mechanics, 94, pp. 275-304.

25. Kannberg, L. D. and Davis, L. R., 1977, An analysis of deep submerged multiple port buoyant discharges, J. of Heat Transfer, Trans. ASME, Vol. 99.

26. Koh, R. C. Y. and Brooks, N. H., 1975, Fluid mechanics of waste water disposal in the ocean, Ann. Review Fluid Mech., 7, 187-211.

27. Koh, R. C. Y. et al., 1974, Hydraulic modeling of thermal outfall diffusers for the San Onofre Nuclear Power Plant, W. M. Keck Lab. of Water Resources and Hydraulics, Tech. Rep. KH-R-30, California Institute of Technology.

28. Lantz, C. H. and Lisauskas, R. A., 1972, Zion discharge model study - Zion Station, Commonwealth Edison Company of Illinois, Alden Research Lab., Tech. Rep.

29. Lee, J. H. W., 1980, Near field mixing of staged diffuser, J. Hydraul. Div., Proc. ASCE, Vol. 106, HY8.

30. Lee, J. H. and Jirka, G. H., 1979, Multiport diffuser as line source of momentum in shallow water, Water Resources Research, Vol. 16, No. 4.

31. Lee, J. H., Jirka, G. H. and Harleman, D. R. F., 1977, Modeling of unidirectional diffusers in shallow water, R. M. Parsons Lab. for Water Resources and Hydrodynamics, Tech. Rep. 228, Massachusetts Institute of Technology.

32. Lee. J. H. W., Jirka, G. H. and Harleman, D. R. F., 1979, Heat recirculation induced by thermal diffusers, J. Hydraul. Div., Proc. ASCE, Vol. 105, HY10.

33. Liseth, P., 1970, Mixing of merging buoyant jets from a manifold in stagnant receiving water of uniform density, Hydraulic Engineering Lab., Tech. Rep. HEL 23-1, University of California, Berkeley, Calif.

34. Lissaman, P. B. S., 1980, The Coriolis program, Oceanus, Vol. 22, No. 4.

35. Morton, B., Taylor, G. I. and Turner, J. S., 1956, Turbulent gravitational convection from maintained and instantaneous sources, Proc. Roy. Soc. A 234, 1-23.

36. Paddock, R. A. and Ditmars, J. D., 1978, An assessment of the once-through cooling alternative for central steam-electric generating stations, Water Resources Research Program, Tech. Rep. ANL/WR-78-5, Argonne National Laboratory.

37. Prandtl, L., 1952, Essentials of Fluid Dynamics, Blackie and Son Ltd.

38. Roberge, J. C., 1976, Optimization of an offshore momentum diffuser in shallow water, Campbell Electric Generating Station, Alden Research Lab., Tech. Rep.

39. Roberts, P. J. W., 1977, Dispersion of buoyant waste water discharge from outfall diffusers of finite length, W. M. Keck Lab. of Hydraulics and Water Resources, Rep. KH-R-35, California Institute of Technology.

40. Roberts, P. J. W., 1979, Line plume and ocean outfall dispersion, J. Hydr. Div., Proc. ASCE, Vol. 105, HY4.

41. Rodi, W., 1975, A review of experimental data of uniform density free turbulent boundary layers, In Studies in Convection, B. E. Launder, Ed., Academic Press.

42. Schijf, J. B. and Schonfeld, J. C., 1953, Theoretical considerations on the motion of salt and fresh water, Proc. Minnesota Int. Hydr. Conv., ASCE and IAHR.

43. Schmidt, F. H., 1957, On the diffusion of heated jets, Tellus, 9, 378-383.

44. Stolzenbach, K. D. et al., 1976, Analytical and experimental studies of discharge designs for the Cayuga Station at the Somerset alternate site, R. M. Parsons Lab. for Water Resources and Hydrodynamics, Tech. Rep. 211, Massachusetts Institute of Technology.

45. Stone and Webster Engineering Corp., 1970, Engineering and ecological studies for design of intake and discharge structures, J. A. FitzPatrick Nuclear Power Plant, Rep. to Power Authority of the State of New York.

46. Tennessee Valley Authority, 1972, Predictions of temperature changes in Wheeler reservoir induced by the discharge of heated water from Browns Ferry Nuclear Power Plant, Adv. Rep. 14, Div. of Water Control Planning, Engineering Lab.

47. Wilson, R. E., 1980, Aerodynamics of wind turbines, In Fluid Mechanics in Energy Conversion, J. D. Buckmaster, Ed., Soc. for Industrial and Applied Mathematics, Philadelphia.

List of Symbols

A = area included by isotherm

A_m = $5 L_D H$ = area of near field mixing zone for alternating diffuser

a_o = nozzle cross-sectional area

B = equivalent slot width

b = local jet or plume width

D = nozzle diameter

F_H = densimetric Froude number of equal counterflow

F_s = $q_o(p_o B^3)^{-1/2}$ = densimetric Froude number of slot discharge

g = gravitational acceleration

g' = buoyant acceleration

H = ambient water depth

h_f = frictional head loss

$I^{1/2}$ = velocity distribution integral for staged diffusers

i = $\sqrt{(-1)}$

J = total kinematic heat flux

j = kinematic heat flux per unit length

k = jet or plume spreading coefficient

L_D = diffuser length

L = half-length of two-dimensional channel model

ℓ = nozzle spacing

M = total kinematic momentum flux

m = kinematic momentum flux per unit length

P = total buoyancy flux

P_e = excess pressure force

p = buoyancy flux per unit length

Q = total volume flux

q = volume flux per unit length

S = bulk dilution under stagnant ambient conditions

S_a = bulk dilution under ambient crossflow

TPL = total pipe length from shore

U_o = discharge velocity

u,v,w = three-dimensional velocities

u_c = jet or plume centerline velocity

V = q_a/q_o = volume flux ratio

x,y,z = Cartesian coordinate system with z upward

x_f = frictional distance for diffuser plume

y_v = virtual source distance for staged diffuser

α = entrainment coefficient

β = nozzle angle relative to diffuser axis

γ = diffuser alignment relative to crossflow

ΔT = excess temperature

ΔT_c = excess temperature at jet or plume centerline

ΔT_{max} = maximum induced excess temperature

$\Delta\rho$ = density difference

λ = bottom friction coefficient

λ_i = interfacial friction coefficient

Φ = $\lambda L_D/H$ = diffuser intermediate field parameter

Φ_c = intermediate field parameter for channel model

ρ = density

θ_o = nozzle angle relative to horizontal

$\theta_o(A)$ = nozzle angle for alternating diffuser

ξ,ζ = complex variables

Subscript

o = discharge condition at diffuser line (or nozzle)

a = ambient conditions

N = conditions within slipstream for unidirectional diffuser

Superscript

* = optimal controlled conditions for alternating diffuser

Table 1

Comparison of Typical Sewage Diffuser and Thermal Diffuser Outfalls Serving a Coastal City of 1 Million Population

Design Variable	Units	Sewage Diffuser	Thermal Diffuser
Total discharge, Q_o	m^3/s (ft^3/s)	8(283)	80(2825)
Relative density deficit, $\Delta\rho_o/\rho_a$	---	0.025 (fresh-salt water)	0.0025 ($\Delta T_o \approx 12°C[22°F]$)
Total buoyancy flux, P_o	m^4/s^3 (ft^4/s^3)	2(230)	2(230)
Discharge velocity, U_o	m/s (ft/s)	5(9.8)	5(9.8)
Total momentum flux, M_o	m^4/s^2 (ft^4/s^2)	40(4630)	400(46300)
Near field dilution requirement, S	---	$\gtrsim$100	$\lesssim$10
Ambient depth, H	m(ft)	50(163)	10(33)
Ambient velocity, u_a	m/s (ft/s)	0.3(1.0)	0.3(1.0)
Diffuser length, L_D	m(ft)	500(1640)	500(1640)
Distributed momentum flux, $\frac{M_o}{L_D H}$	m^2/s^2 (ft^2/s^2)	0.0016(0.017)	0.08(0.85)
Order of magnitude of induced velocities, $O\{(\frac{M_o}{L_D H})^{1/2}\}$	m/s (ft/s)	0.04(0.1)	0.3(1.0)

Table 2

Diffuser Design Comparison: Summary of Environmental Impact Measures

DIFFUSER TYPE	STAGNANT OR NEAR-STAGNANT				AMBIENT CURRENT		
	Temperature exceedance areas		Induced velocities	Comments	ΔT		Comments
	ΔT_{max} = 1.5°C (2.7°F)	$\frac{1}{2}\Delta T_{max}$ = 0.75°C (1.4°F)			u_a = 0.1 m/s (0.3 ft/s)	u_a = 0.3 m/s (1 ft/s)	
UNIDIRECTIONAL	< 3 ha (7 ac) Fig. 11	35 ha (85 ac) Fig. 11	0.63 m/.s (2.1 ft/s) Eq. 6	Concentrated vertically fully mixed flow field. Bottom temperature impact.	1.3°C (2.3°F) Eq. 15*	0.9°C (1.7°F) Eq. 15*	*For coflowing design (suitable for non-reversing conditions). Tee design unsuited for current conditions.
STAGED	negligible	45 ha (110 ac) Fig. 15	0.63 m/s (2.1 ft/s) Eq. 18	Concentrated vertically fully mixed flow field. Bottom temperature impact.	0.7°C (1.3°F) Eq. 22	0.4°C (0.7°F) Eq. 22	Suitable for current reversals.
ALTERNATING	6 ha (15 ac) Fig. 22	120 ha (300 ac) Fig. 22	small	Stratified flow field. Minimal bottom temperature impact.	0.7°C (1.3°F) Eq. 36	0.3°C (0.5°F) Eq. 36	Suitable for current reversals.

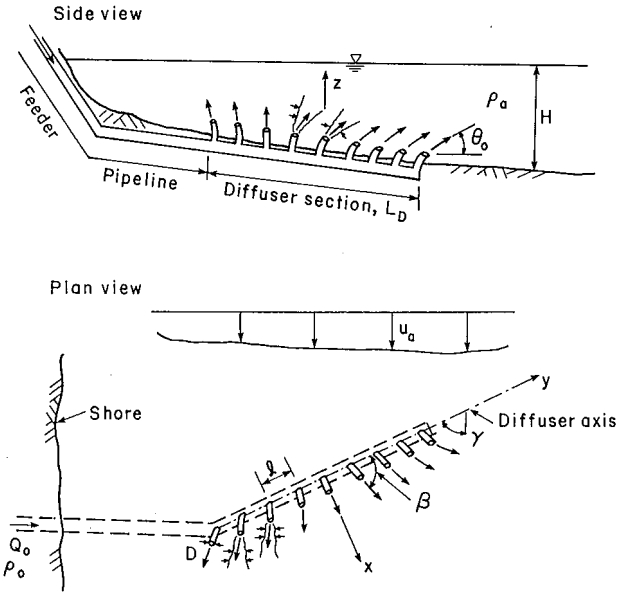

Figure 1. Submerged Multiport Diffuser: Definition Diagram

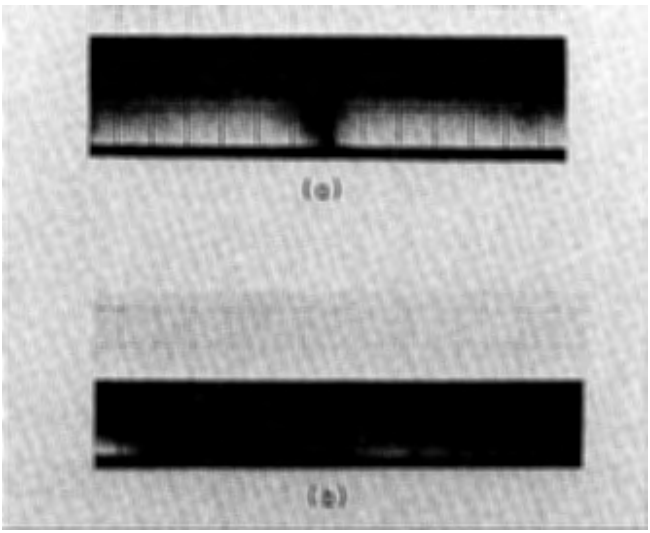

Figure 2. Vertical Buoyant Line Jet Discharging Into Finite Depth. a) Stable Discharge Configuration. b) Unstable Discharge With Recirculation Zone. (From 24).

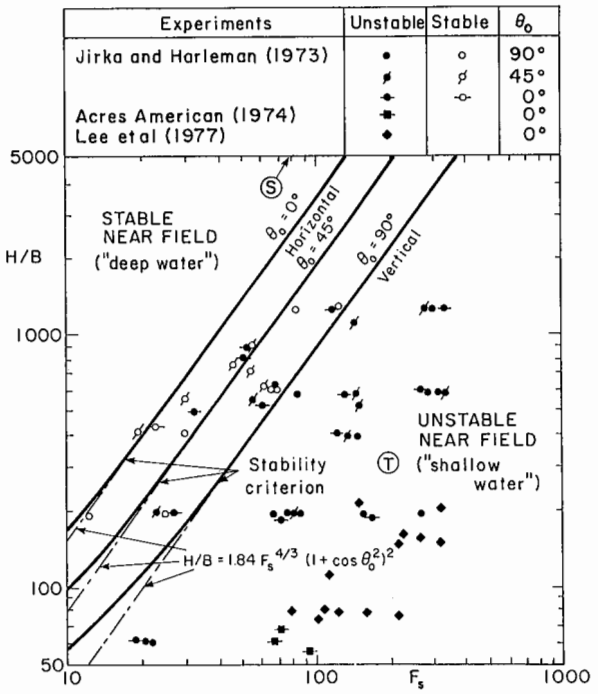

Figure 3. Two-Dimensional Channel Approximation of General Three-Dimensional Diffuser Flow Field.

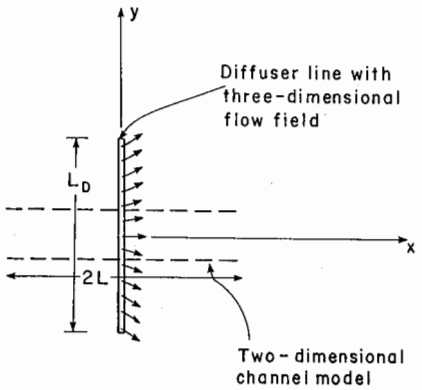

Figure 4. Stability Diagram for Line Buoyant Discharges Into Confined Stagnant Ambient.

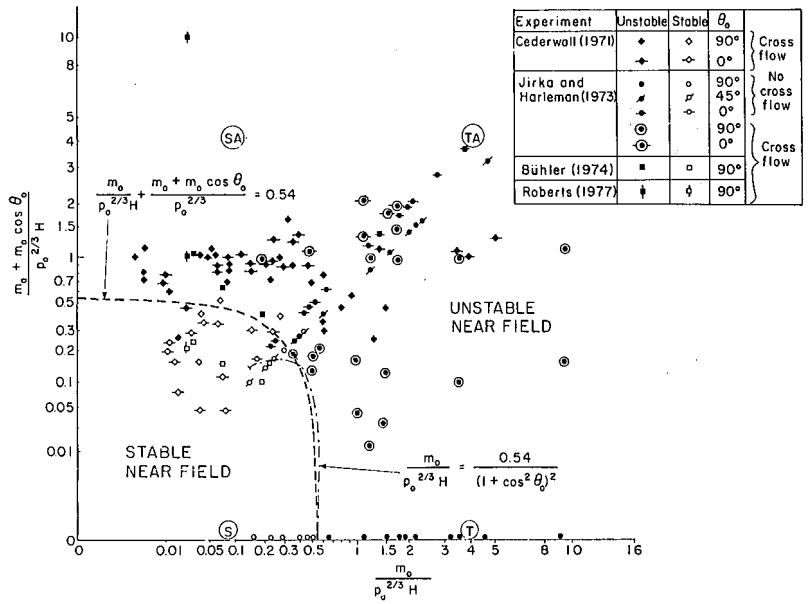

Figure 5. General Stability Diagram for Line Buoyant Discharges Into Confined Depth Comprising Stagnant and Flowing Ambient.

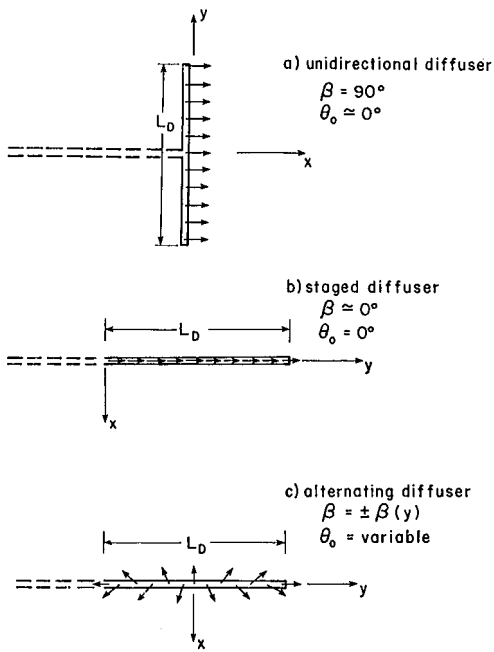

Figure 6. Nozzle Geometries for Three Major Diffuser Types.

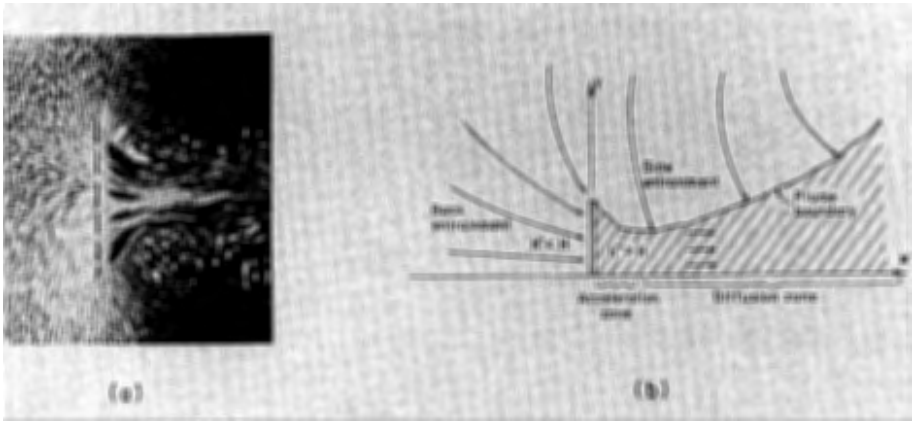

Figure 7. Flow Field Induced by Unidirectional Diffuser: a) Surface Flow Pattern Observed In Experiment (Adapted From 7, 30). b) Structure Of Diffuser Plume.

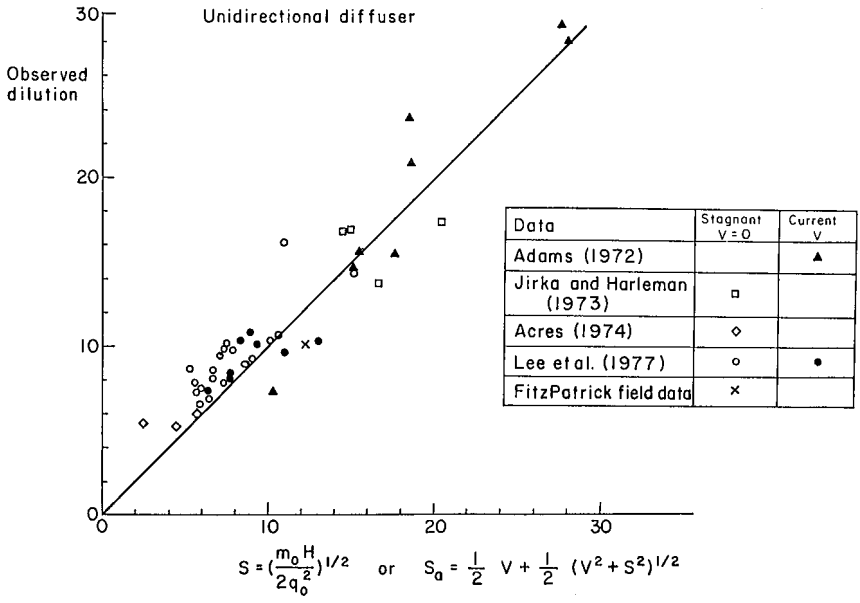

Figure 8. Unidirectional Diffuser: Comparison Of Observed and Predicted Bulk Dilution for Stagnant (S) and Flowing (S_a) Ambient.

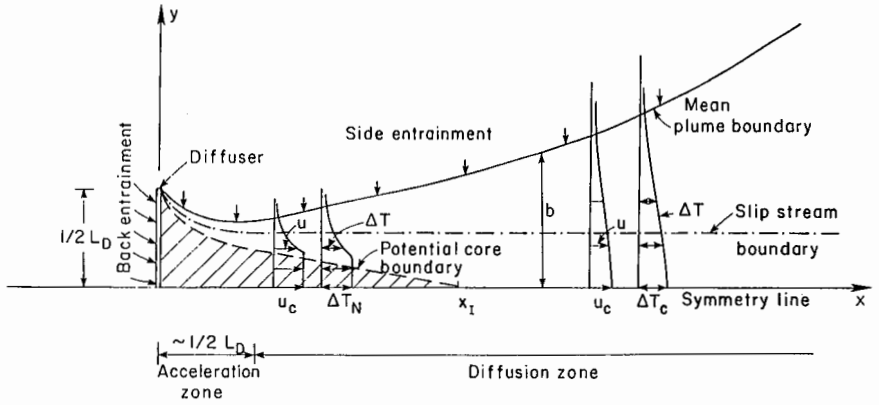

Figure 9. Details of Intermediate Field Plume For Unidirectional Diffuser.

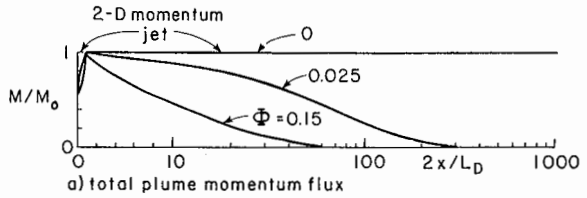

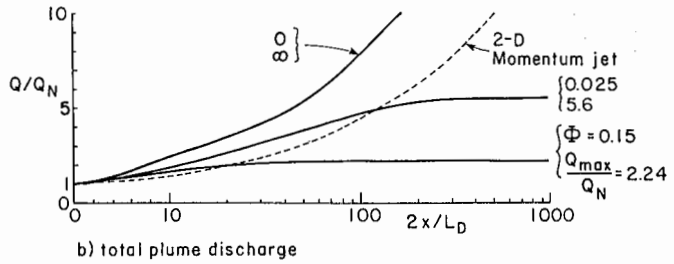

Figure 10. Momentum Flux and Discharge Within Intermediate Field Plume of Unidirectional Diffuser. (From 30)

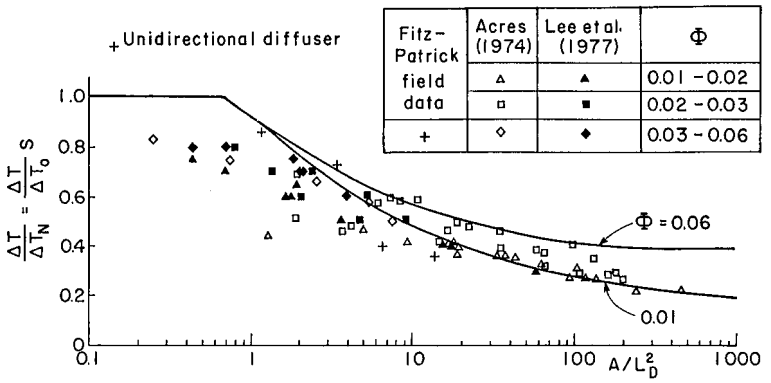

Figure 11. Unidirectional Diffuser: Comparison of Observed and Predicted Excess Isotherm Areas for Stagnant Ambient.

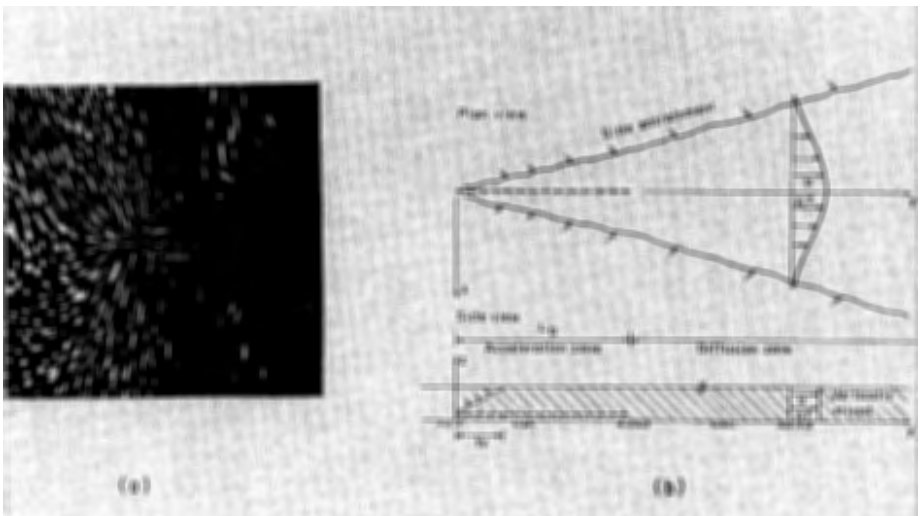

Figure 12. Flow Field Induced by Staged Diffuser: a) Surface Flow Pattern Observed in Experiment (Adapted From 7, 8). b) Structure of Diffuser Plume.

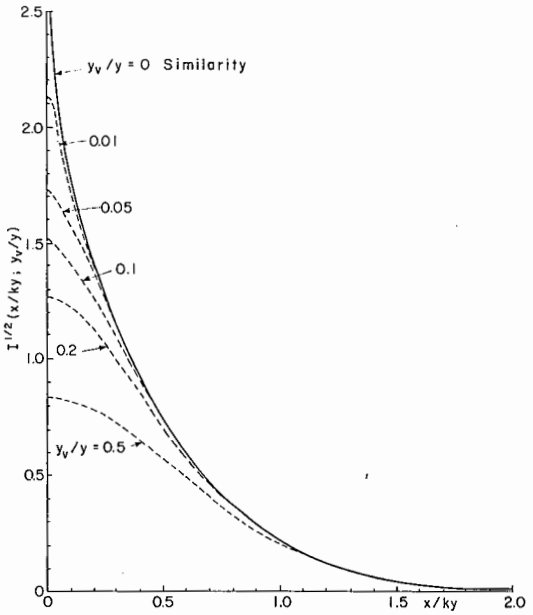

Figure 13. Staged Diffuser: Normalized Lateral Velocity Distributions. Solid Line Gives Asymptotic Self-Similar Distribution, Eq. 17; Dashed Lines Give Evolving Distributions With Initial Virtual Source Effect.

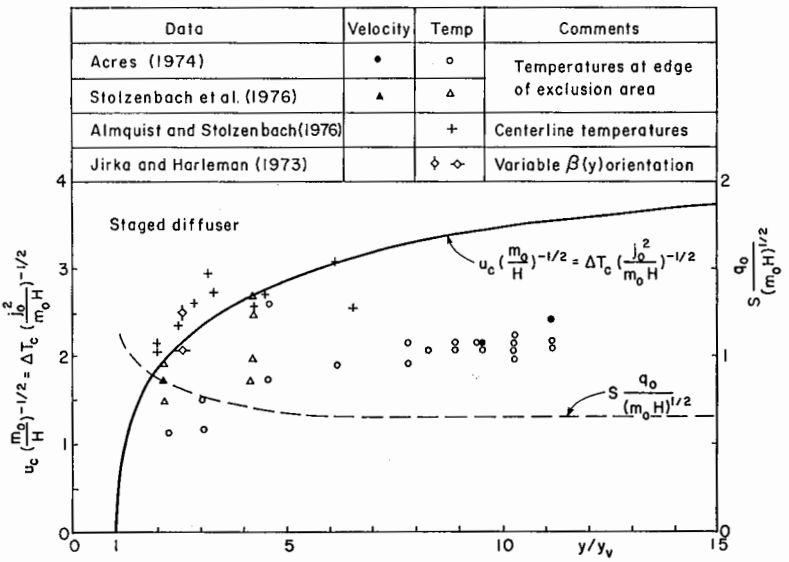

Figure 14. Staged Diffuser: Comparison of Predicted and Observed Centerline Temperatures and Velocities, Respectively, and Prediction of Bulk Dilution.

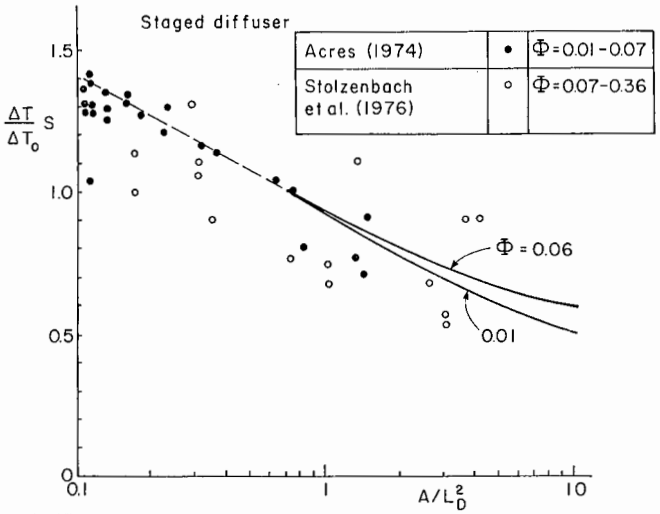

Figure 15. Staged Diffuser: Comparison of Observed and Predicted Isotherm Areas for Stagnant Ambient.

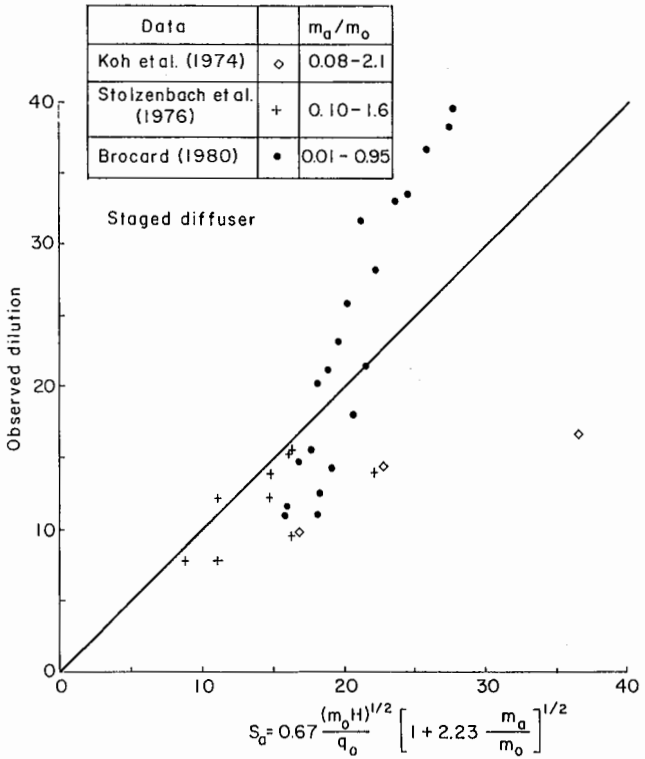

Figure 16. Staged Diffuser: Comparison of Observed and Predicted Dilutions Under Ambient Current Conditions.

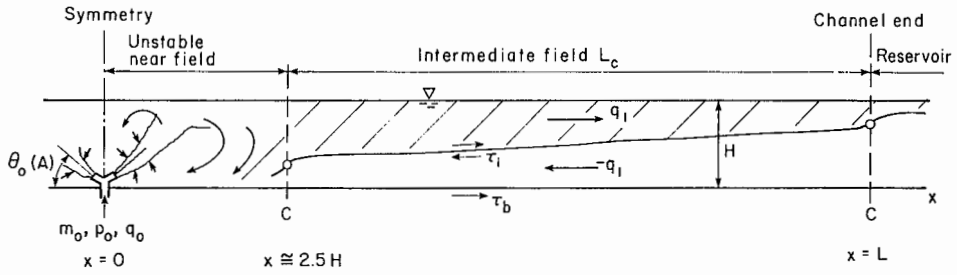

Figure 17. Alternating Diffuser: Stratified Counterflow Characteristics In Two-Dimensional Channel Model.

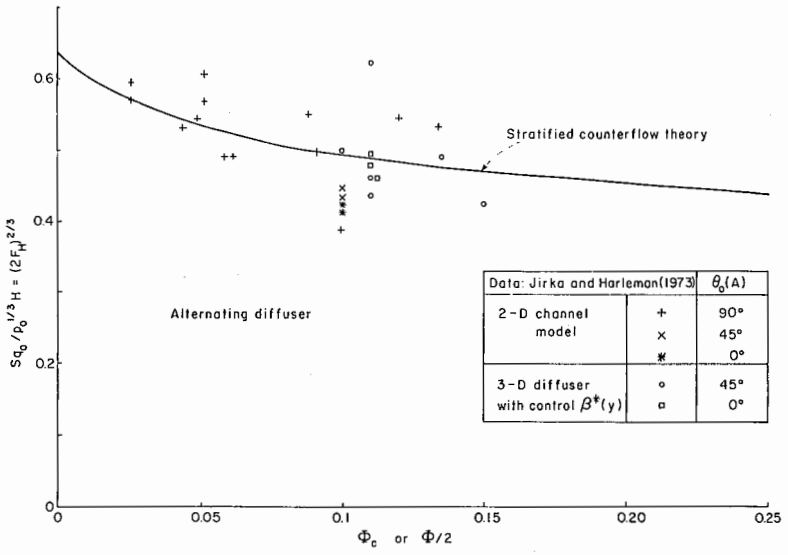

Figure 18. Alternating Diffuser: Predicted Dilutions In Comparison With Experiments in Two-Dimensional Channel (Φ_C) and With Controlled Three-Dimensional Diffuser ($\Phi/2$).

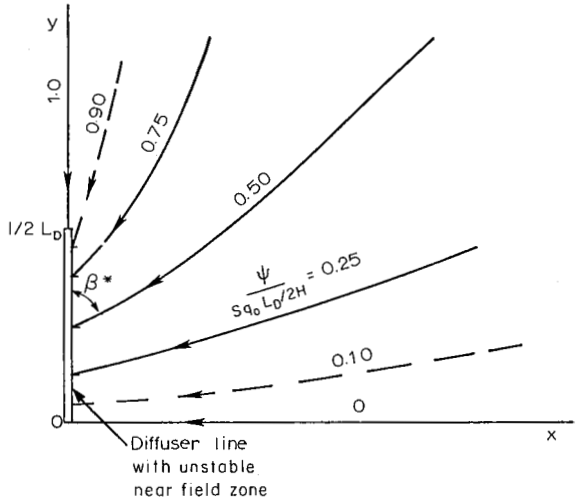

Figure 19. Sink Flow Velocity Field In Lower Layer of Alternating Unstable Diffuser With Nozzle Control.

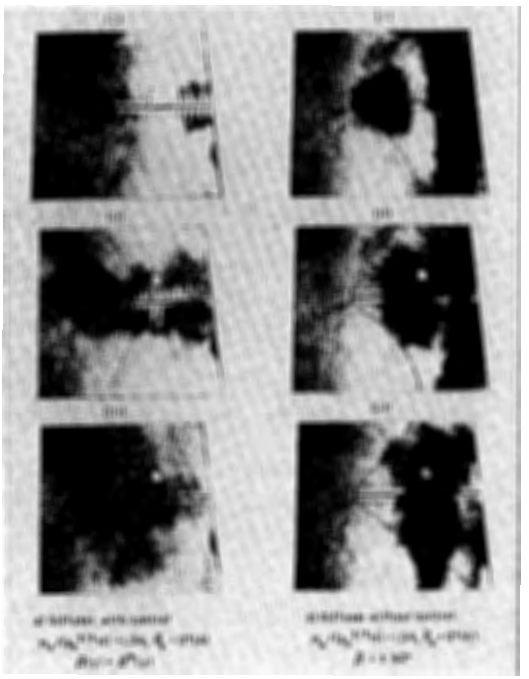

Figure 20. Alternating Diffuser: Effect of Nozzle Control Demonstrated By Dye Release Into Steady State Flow Field In Half Plane. a) Diffuser With Control. b) Diffuser Without Control.

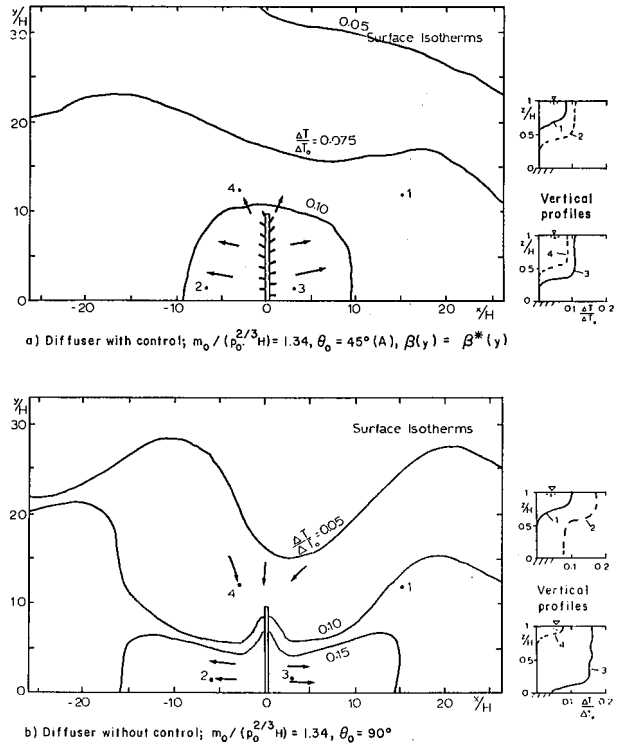

Figure 21. Alternating Diffuser: Effect of Nozzle Control on Temperature Field. a) Diffuser With Control. b) Diffuser Without Control.

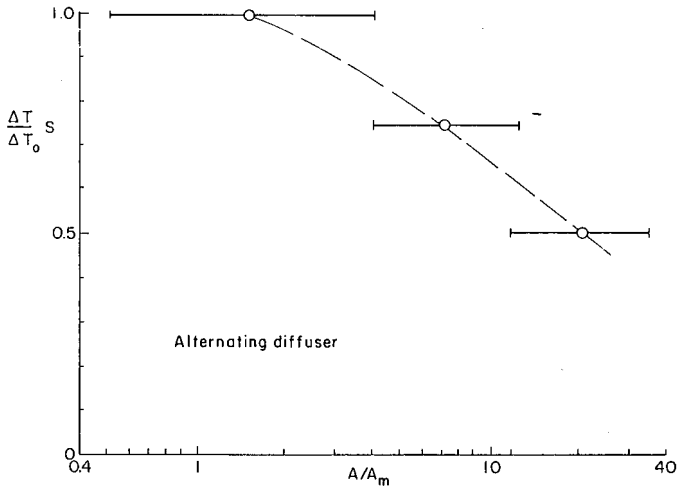

Figure 22. Alternating Diffuser: Additional Temperature Reduction In the Intermediate Field. Experiments By Jirka and Harleman (23).

Diffuser Input of Horizontal Momentum	Nozzle Characteristics	Flow Field in First Quadrant	Comments
Deficit of y-momentum	$\beta(y) > \beta^*(y)$ or $\theta_o(A) > \theta_o^{max}(A)$	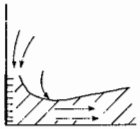	Fully mixed counter clockwise circulation; similar to "unidirectional diffuser"
"Diffuser control" Balanced y-momentum	$\beta(y) = \beta^*(y)$ and $\theta_o(A) < \theta_o^{max}(A)$	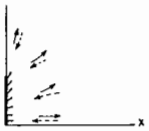	Weak stratified counterflow in all directions; "alternating diffuser"
Surplus of y-momentum	$\beta(y) < \beta^*(y)$ and $\theta_o(A) < \theta^{max}(A)$	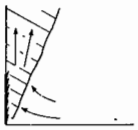	Fully mixed clockwise circulation; "staged diffuser"

Figure 23. Generic Flow Fields For Shallow Water Diffusers As a Function of Discharge Momentum Distribution.

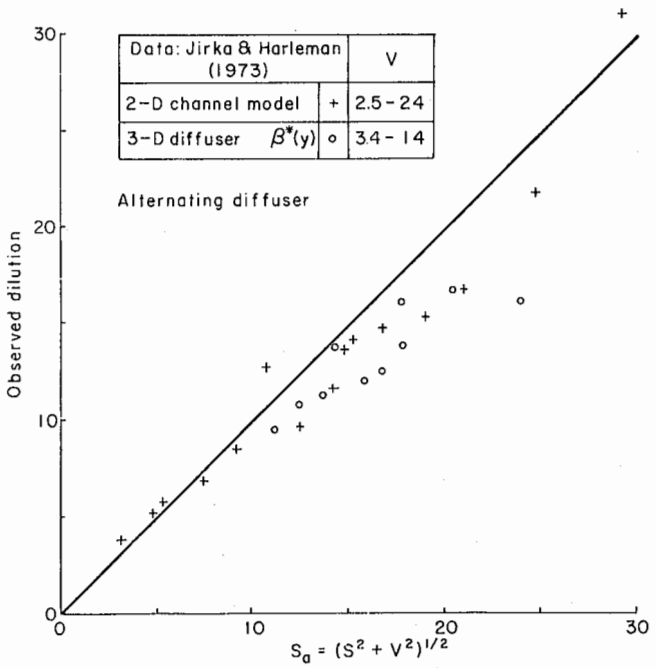

Figure 24. Alternating Diffuser: Comparison of Predicted and Observed Dilutions Under Ambient Current Conditions.

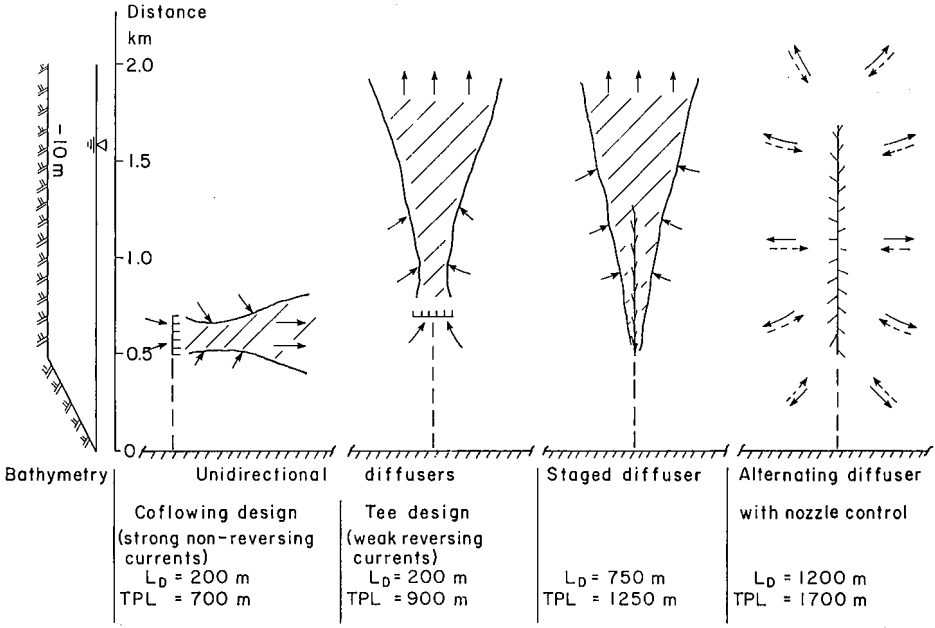

Figure 25. Design Comparison For Diffusers In Coastal Environment.